Fabrication and Characterization of Mechanically Strong Hydrogel Using Modified Nano-Starch Cross-linker

A thesis submitted in partial fulfillment of the requirement for

the degree of M.Sc. in Chemistry

SUBMITTED BY

Tarun Kante Majumder

STUDENT ID: 0416032707

SESSION: April 2016

Soft and Smart Materials Research Group
Department of Chemistry
Bangladesh University of Engineering & Technology,
Dhaka-1000.

March, 2019

YEAR OF DEFENSE 2019

The thesis entitled 'Fabrication and Characterization of Mechanically Strong Hydrogel Using Modified Nano-Starch Cross-linker, submitted by Tarun Kante Majumder, Roll No.:0416032707 Session: April-2016, has been accepted as satisfactory in partial fulfillment of the requirement for the degree of Master of Science (M. Sc.) in Chemistry on 23.03.2019.

BOARD OF EXAMINERS

1. Dr. Abu Bin Imran Associate Professor Department of Chemistry, BUET, Dhaka (Supervisor)	Chairman
2. Dr. Md. Abdur Rashid Professor & Head Department of Chemistry, BUET, Dhaka	Member (Ex-Officio)
3. Dr. Md. Shakhawat Hossain Firoz Professor Department of Chemistry, BUET, Dhaka	Member
4. Dr. Md. Abu Bin Hasan Susan Professor Department of Chemistry, University of Dhaka, Dhaka-1000	Member (External)

Declaration by the candidate

It is hereby declared that this thesis or any part of it has not been submitted elsewhere for the award of any degree or diploma.

……..

Tarun Kante Majumder

DEDICATED TO

MY BELOVED FAMILY

&

HONORABLE SUPERVISOR

Table of Contents

List of Figures and Tables…….. viii

List of Abbreviations of Technical Symbols and Terms…… xi

Acknowledgement…….. xii

Abstract……... xiv

CHAPTER 1: Introduction……... 1

1.1 Starch…….. 1

1.2 Introduction of Natural Starch……... 1

1.2.1 Compositions of Natural Starch……. 1

1.2.2 Corn Starch……. 4

1.2.3 Wheat Starch…….. 5

1.2.4 Tapioca Starch…… 5

1.2.5 Potato Starch…….. 5

1.3 Composite Material…… 6

1.4 Nanocomposite Material…… 7

1.4.1 Polymer-matrix Nanocomposite…… 7

1.4.2 Application of Nanocomposite…….. 7

1.5 Hydrogel……. 8

1.5.1 Hydrogels and Their Properties……. 8

1.6 Mechanical Properties of Hydrogels……. 9

1.6.1 Tensile Strength……. 10

1.6.2 Stress-Strain Diagram…… 11

1.6.3 Young‟s Modulus of Elasticity…….. 11

1.7 Biodegradability and Surface Properties of Hydrogels…….. 11

1.7.1 Permeability of Hydrogels……. 12

1.7.2 Stimuli Responsive Hydrogels……... 12

1.7.3 pH responsive Hydrogel……. 13

1.7.4 Temperature Responsive Hydrogel…… 13

1.8 Applications of Hydrogels……. 14

1.9 Cross-linker…… 14

1.9.1 Significance of Crosslinking……. 15

1.9.2 Hydrogels and Crosslinking……... 16

1.10 Literature Review……... 18

1.10.1 The aim of the Current Research……... 19

Reference……. 20

CHAPTER 2: Experimental……. 28

2.1 Materials and Instruments…….. 29

2.1.1 Chemicals and Reagents…… 29

2.1.2 Instruments……. 30

2.2 Methods of Preparation…….. 30

2.2.1 Synthesis of Nano-starch Particles (NSP)…… 30

2.2.2 Synthesis of Carboxylated Nano-starch (CNS)……. 31

2.2.3 Synthesis of Modified Nano-starch Cross-linker (MNSC)…… 32

2.2.4 Synthesis of Hydrogels Using Modified Nano-starch Cross-linker (MNSC)... 33

2.3 Fourier Transform Infrared Analysis (FTIR)……. 35

2.4.1 Field Emission Scanning Electron Microscopy (SEM)……. 36

2.4.2 Energy Dispersive X-Ray Analysis (EDS)……... 36

2.5 Nuclear Magnetic Resonance (NMR) Spectroscopy……. 36

2.6 Mechanical Properties of Hydrogel……... 36

References……... 38

CHAPTER 3: Results & Discussion…… 39

3.1 Synthesis of Nano-starch Particle ……..... 40

3.2 Surface Morphology Study of Nano-starch Particle Using Scanning Electron Microscope…… 41

3.3 Energy-Dispersive X-ray Spectroscopy Analysis of Nano-starch Particle……... 43

3.4 Carboxylated Nano-starch Particle Preparation…… 44

3.5 Synthesis of Modified Nano-starch Cross-linker ……..... 45

3.5.1 Study of Surface Morphology of MNSC Using Field Emission Scanning Electron Microscopy ……. 46

3.5.2 Energy-Dispersive X-ray Spectroscopy Analysis of MNSC……..... 46

3.6 Functional Group Investigation by Fourier Transform Infrared Spectroscopy ……... 47

3.7 Nuclear Magnetic Resonance Analysis……. 50

3.8 Synthesis of Modified Nano-starch Cross-linker Based Poly (*N*-isopropylacrylamide) (MNSC-NIPA) Hydrogel……... 51

3.8.1 General Reaction Mechanism of Free Radical Polymerization for MNSC-NIPA hydrogel……... 52

3.9 Mechanical Properties of MNSC-NIPA hydrogels……... 55

3.9.1 Mechanical Properties of MNSC-NIPA Hydrogels for Elongation…….. 55

3.9.2 Mechanical Properties of MNSC-NIPA Hydrogels for Compression……... 61

References……... 67

CHAPTER 4: Conclusion…… 70

List of Figures and Tables

Figures

Figure 1.1 Chemical structure of amylose and amylopectin…….. 2

Figure 1.2 Single helix structure of amylose…….. 3

Figure 1.3 Structure of branched amylopectin……... 3

Figure 1.4 Typical stress-strain curve of materials…… 11

Figure 1.5 The pH-responsive swelling of (a) anionic and (b) cationic hydrogels… 13

Figure 1.6 Cross-linking in polymer…….. 16

Figure 2.1 Schematic representation of synthesis of nano-starch particles from micro-starch…….. 31

Figure 2.2 Schematic representation of carboxylated nano-starch particles…….. 32

Figure 2.3 Schematic illustration of preparation of MNSC……..... 33

Figure 2.4 Schematic representation of MNSC-NIPA hydrogel…… 35

Figure 3.1 Schematic representation of nano-starch particle formation…… 40

Figure 3.2 SEM image of (a) MSP with magnification x 500 (b) NSP with Magnification x 50000 and (c) NSP with magnification x 30000……... 42

Figure 3.3 EDS spectra of NSP ……..... 43

Figure 3.4 Formulae for oxidation of primary hydroxyl groups of nano-starch to carboxylated nano-starch particles via TEMPO-mediated oxidation….. 44

Figure 3.5 Schematic representation of the structure of a modified nano-starch cross-linker……... 45

Figure 3.6 SEM image of a) MNSC with magnification x 30,000 and b) MNSC with magnification x 50,000……. 46

Figure 3.7 EDS spectra of MNSC…….. 47

Figure 3.8 FTIR spectra of nano-starch particle, carboxylated nano-starch, modified nano-starch cross-linker……. 48

Figure 3.9 FTIR spectra of modified nano-starch cross-linker after magnification in the region of 1600-1700 cm^{-1}…… 49

Figure 3.10 Structure of MNSC cross-linker (One glucose unit is depicted for clarity)……... 50

Figure 3.11 ^{1}H-NMR spectrum of synthesized MNSC cross-linker…… 51

Figure 3.12 Reaction mechanism of free radicle polymerization for MNSC-NIPA hydrogel…… 53

Figure 3.13 Chemical structure of MNSC-NIPA hydrogel (For the sake of clarity only one glucose unit is depicted)……. 54

Figure 3.14 Elongation process of MNSC-NIPA hydrogel……. 56

Figure 3.15 Stress-strain curves of MNSC-NIPA hydrogel for elongation……. 57

Figure 3.16 Tensile strength and Young‟s Modulus of MNSC-NIPA hydrogel during elongation…….. 58

Figure 3.17 Elongation of break of MNSC-NIPA hydrogel…… 59

Figure 3.18 Toughness of MNSC-NIPA hydrogel for elongation……... 60

Figure 3.19 Compressive test of MNSC-NIPA hydrogel……. 62

Figure 3.20 Compressive stress-strain curve MNSC-NIPA hydrogel……. 62

Figure 3.21 Compressive strength of MNSC-NIPA hydrogel……. 63

Figure 3.22 Young‟s Modulus of MNSC-NIPA hydrogel during compression……. 64

Figure 3.23 Toughness (Jm^{-3}) of MNSC-NIPA hydrogel for compression……. 65

Tables

Table 1.1 Some typical hydrogels, their cross-linking agents and applications……. 17

Table 2.1 Composition of different hydrogel precursors……... 34

Table 3.1 EDS elemental analysis of NSP……. 43

Table 3.2 EDS elemental analysis of MNSC……. 47

Table 3.3 Characteristic bands of NSP, CNS and MNSC in FT-IR spectra…….. 49

Table 3.4 Tensile strength and Young‟s modulus of MNSC-NIPA hydrogel……... 58

Table 3.5 Elongation of break for MNSC-NIPA hydrogel…… 59

Table 3.6 Toughness for MNSC-NIPA hydrogel……... 61

Table 3.7 Compressive strength of MNSC-NIPA hydrogel……... 63

Table 3.8 Young‟s Modulus of MNSC-NIPA hydrogel…… 65

Table 3.9 Toughness for MNSC-NIPA hydrogel……..... 66

List of abbreviations of technical symbols and terms

1. Micro-Starch particle (MSP)
2. Nano-Starch particle (NSP)
3. Carboxylated Nano-Starch (CNS)
4. Tetramethylethylenediamine (TEMED)
5. Modified Nano-Starch Crosslinker (MNSC)
6. 1-Ethyl-3-(3-dimethylaminopropyl)-carbodiimide (EDC)
7. 2, 2, 6, 6-tetramethylpyperidine-1-oxyl (TEMPO)
8. 2-Aminoethyl methacrylate hydrochloride (2-AEM)
9. Poly (*N*-isopropylacrylamide) (PNIPAAM)
10. Potassium per sulfate (KPS)
11. *N*-isopropylacrylamide (NIPAAM)
12. Modified Nano-Starch Crosslinker-*N*-isopropylacrylamide (MNSC-NIPA) hydrogel

Acknowledgement

At the beginning, I humbly acknowledge my deepest gratitude to the Almighty, the most gracious, benevolent and merciful creator for his infinite mercy bestowed on me to complete the research work presented in the dissertation.

It is an immense pleasure for me to acknowledge my honest sense of gratitude, sincere appreciation, heartfelt indebtedness and solemn regards to my reverend teacher and supervisor Dr. Abu Bin Imran, Associate Professor, Department of Chemistry, Bangladesh University of Engineering and Technology (BUET), for his kind supervision, indispensable guidance, valuable and constructive suggestions, liberal help and continuous encouragement during the whole period. In fact, I am quite lucky to be a part of his ambitious research team.

It is my great honor to convey my sincere gratitude to my respected teacher Professor Dr. Md. Abdur Rashid, Honorable Head, Department of Chemistry, BUET for giving me his wonderful support to move through the academic processes during this M.Sc. program. I would like to convey my deepest gratitude to Professor Dr. Md. Shakhawat Hossain Firoz, Dr. Chanchal Kumar Roy and Dr. Md. Ayub Ali of the Department of Chemistry, BUET, for their valuable suggestions, comments, guidance and help during the research period.

I am also thankful to all other respected teachers of the Department of Chemistry, BUET, for their continuous support. I would also like to thank all of the officers and staffs of the Department of Chemistry, BUET for their relentless help during my study period. I am highly grateful to all members of the board of examiners for their valuable suggestions and comments.

I am thankful all of the members of Soft and Smart Materials Research Group for their friendly cooperation and lovely encouragement throughout my research period. My special thanks to Aminur Rahman, H. B. Muhammad Zukaul Islam, Noman Chowdhury, and Rezaul Karim Reza for their continuous help during the research.

I am grateful to Department of Glass and Ceramics Engineering, Bangladesh University of Engineering and Technology for the sample characterizations of FE-SEM and EDS during my research.

Finally, I would like to express my heartfelt indebtedness and profound gratitude to my beloved father, mother and all of my family members for their continuous inspiration and immeasurable sacrifices throughout the period of my study.

March, 2019 Tarun Kante Majumder

Abstract

Hydrogels are hydrophilic three-dimensional highly cross-linked polymer which has wide applications in a variety of fields but the inherent weak mechanical properties make them unsuitable for many practical applications. In addition, most of the cross-linker are used for the synthesis of conventional chemical hydrogels are toxic in nature and non-biodegradable. This work aim at facile fabrication of mechanically strong and biodegradable hydrogel using a chemically cross-linked nano-starch as a cross-linker. Here, we employ a uniform dispersion of nanoparticles for the synthesis of hydrogels using different amount of vinyl modified nano-starch cross-linker (MNSC). Mechanically strong hydrogel is prepared by free radical polymerization of *N*-isopropylacrylamide (NIPAAM) monomer in presence of MNSC as a cross-liking agent and potassium persulfate (KPS) as redox initiator. First, nano-starch particle (NSP) is synthesized from micro starch granules via acid hydrolysis. The synthesized NSP is then converted to carboxylated nano-starch particle (CNS) using 2,2,4,4-tetramethyl-1-oxyalpiperidine (TEMPO) mediated selective oxidation of NSP. MNSC cross-linker is synthesized by the coupling reaction between CNS and 2-Aminoethyl methacrylate hydrochloride (2-AEM) in presence of coupling agent *N*-(3-dimethylaminopropyl)-*N*-ethylcarbodiimide hydrochloride (EDC). The synthesized MNSC are able to act as cross-linker during free radical polymerizations of NIPAAM. The surface morphologies of NSP and MNSC are observed by the scanning electron microscopy (SEM) images. The superior mechanical properties of the hydrogels are established by the Universal Testing Machine (UTM) at room temperature. Here, MNSC-NIPA hydrogels can be prepared only by using a small amount of MNSC to overcome the inherent poor mechanical properties of the traditionally cross-linked polymeric hydrogels.

CHAPTER-1

Introduction

1.1 Starch

Starch is a naturally occurring, biodegradable, inexpensive and abundant polysaccharide molecule. It is widely distributed in the form of tiny granules as the major reserve carbohydrate in stems, roots, grains, and fruits of all forms of green leafed plants. Cereal grains, such as corn, wheat, sorghum, and tubers, and roots, such as potato, tapioca, arrowroot, etc., are some of the commercial sources of starch for industrial exploitation. It consists of glucose units $(C_6H_{10}O_5)_n$ with n ranging from 300 to 1000. It can be produced at low cost and at large scale. Starch is not a real thermoplastic material but, in presence of a plasticizer, high temperatures and shearing, it melts and fluidizes, like thermoplastic polymer. We, therefore, choose starch as a raw material in this work.

1.2 Introduction of natural starch

Starch is a carbohydrate material that can be hydrolyzed into small molecules by specific enzymes during animal metastasis, generating biological energy for animals. Many plants, in their fruits, seeds, tubers or rhizomes, grow with starch. Potato, corn, wheat and rice are major resources for production of starch worldwide.

1.2.1 Compositions of natural starch

Starch contains two major components: one is amylose, which is a linear polymer, and the other is amylopectin, which is a highly branched polymer. The repeat units in both amylose and amylopectin are identical (so-called α-D-glucosyl residues) but connected in different ways, as given in Figure 1.1 Most starch contains 20—30 wt % of amylose, although some waxy starches contain very little amylose. In amylose, *α-D*-glucosyl residues are linked by an α [1→4] bond. Typically, the molecular weights of extracted amylose are in the order of 105—106 g/mol [1]. Amylose generally is recognized as linear macromolecule. However, it has been reported that there is a slight degree of branching (9—20 branch points per molecule) in amylose from various botanical sources [2]. The length of side chains ranges from 4 to over 100 repeat units [3]. There is no effective way of separating the branched amylose from the linear amylose. Side chains on branched amylose form small clusters rather than a random comb structure. Note that amylopectin also forms clusters by its branched side chains, which will be elaborated on later. Branched amyloses have iodine binding capability but amylopectin does not have. In

aqueous solutions, amylose molecules can form extended chains with a hydrodynamic radius of 7-22 nm. In natural starch, the amylose molecules tend to have a rather stiff left-handed single helical structure or form an even stiffer parallel double left-handed helix [4].

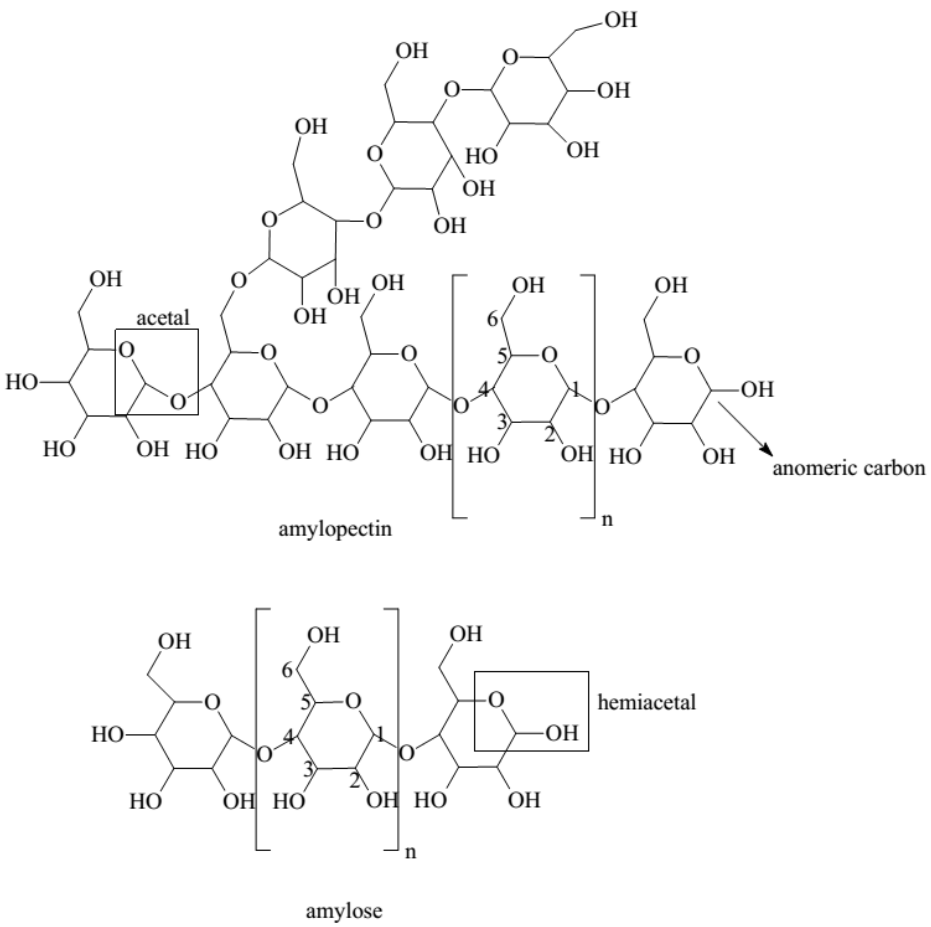

Figure 1.1: Chemical structure of amylose and amylopectin

The helix consists of six *α-D*-glucosyl residues per turn with a pitch of 0.8 nm. Figure 1.2 shows a single helix structure of amylose molecule. On each of the glucose residues, hydroxyl groups connecting with carbons on position 2 and 6 (C2 and C6) point outward of the helix, while the hydroxyl group connecting with carbon on position 3 (C3) points inward of the helix, which makes the inner surface of the helix more hydrophobic than the outer surface. Thus, amylose with a helix structure can hold the hydrocarbon portion of glycerides and fatty acid in its helix cavity to form a V-helix complex. The distinct capability of amylose to bind with iodine is also by holding iodine ions in its hydrophobic helix cavity. Amylopectin is a highly branched component of starch. The *α-D*-glucosyl residues are mainly linked by α [1→4] bonds but with 5-6% of α [1→6] bonds at the branch points. Its molecular weight ranges 107-109 g/mol.

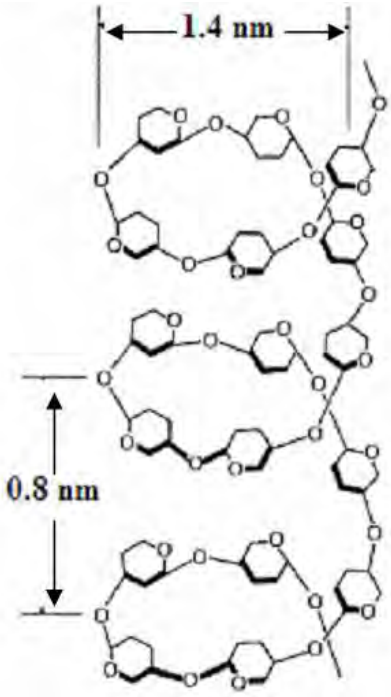

Figure 1.2: Single helix structure of amylose.

The amylopectin molecular chains can be classified into three categories by their ways of connecting with each other: the C chain carries the sole reducing end of the molecule; the A chain (unbranched) is only linked to the rest of the molecule through its potential reducing end; and the B chains carry one or more A chains and/or B chains. Figure 1.3 shows a schematic description of this classification.

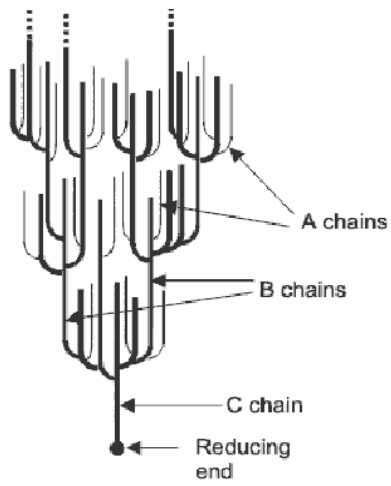

Figure 1.3: Structure of branched amylopectin

In most experiments, the C chain is not distinguished from B chains. According to their positions in the cluster structure, B chains are further subdivided: B_1 is a short chain, being components of only one cluster while B_2, B_3, etc. are long chains that span over two, three, or more clusters, thereby interconnecting them. The branching points on the amylopectin molecules are not randomly distributed but periodically clustered. The distance between two clusters on the same B chains is 2-2-*α*-*D*-glucosyl residues on average. Most short chains (the average degree of polymerization ranges from 14 to 18) are organized within clusters, while long chains (the average degree of polymerization is more than 55) usually span more than one cluster. The molar ratio of short to long chains, influenced by the source of starch, varies from 5 in potato starch amylopectin to 8—10 in cereal amylopectin. The distribution of chain length in amylopectin critically influences the inner assembly structure of starch granules and the interaction with the water or solvent.

1.2.2 Corn starch

The word „corn" is used in the United States as the common name for the cultivated member of the grass family (Gramineae) known to botanists as Zeamaysl. More specifically, „corn" means the seed produced by this plant. Outside of the United States, this crop is commonly known as maize. The mature corn kernel is composed of four principle parts: tip cap, 0.8%; pericarp, 5.3%; germ, 11.9%; and endosperm, 82%. The most important genetic change in corn for starch production was development of waxy maize (corn) hybrids. Starch from waxy maize, which contains 100% of the branched starch fraction, amylopectin, has become a major food starch. This corn must be grown in fields isolated from dent corn to prevent crosspollination, and generally will be grown under identity-preserved contracts to ensure delivery of uncontaminated shipments of maize to the wet-milling establishment and to provide adequate supply. The milling properties of waxy maize are similar to those of regular corn, except that the yield of soluble is a little higher, starch yield is lower and starch and gluten slurries filter and dry a little more slowly than those from normal dent corn. This characteristic has been shown to be caused by the presence of a small amount of a phytoglycogen. The addition of a small amount of an amylolytic enzyme to the slurries results in normal filtering and drying characteristics [5]. High-amylose corn having starch which contains 55 – 80% of the linear starch fraction, amylose, has also been developed [6] and must also be grown under contract. Production of amylomaize is even smaller than it is for waxy hybrids because of

limited uses for the starch. Starch yields of high-amylose corn are lower than those of dent corn [7].

1.2.3 Wheat starch

Starch comprises 54-72% of the dry weight of wheat kernels [8-9]. Starch content is positively associated with grain yield, but inversely related to protein content [10-12]. Normal wheat starch is comprised of 25% amylose and 75% amylopectin. Amylose is a mixture of linear and lightly branched (0.2 – 0.8% of linkages) molecules having a number average degree of polymerization of 1000 – 5000, whereas amylopectin is monodisperse and highly branched (4 –6% of linkages) with a DP of about 10 000 or more. The detailed structural features of amylose and amylopectin are dependent on the source of starch, even among wheats. Moreover, the proportions of amylose and amylopectin in starch may vary within a plant source, due to genetic mutation. Amylose and amylopectin are readily isolated and purified, but branched and linear amylose molecules from wheat starch have not been separated and isolated.

1.2.4 Tapioca starch

Tapioca starch is obtained from the roots of the cassava plant, which is found in equatorial regions between the Tropic of Cancer and the Tropic of Capricorn. Typically, cassava starch contains 17 – 20% amylose. Unlike corn (0 – 70% amylose content) and rice (0 – 40% amylose content), no significant variation of amylose content has been found in cassava starch. Similar to other starches, the amylase molecules of cassava starch are not completely unbranched as indicated by their beta-amylolysis limit, a value lower than that for corn, potato, rice and wheat starches. In addition, cassava amylose has a higher molecular weight than other starches. Each fraction can be classified in terms of its chain length (degree of polymerization, DP) and position in amylopectin molecules [13].

1.2.5 Potato starch

In some potato starch applications, as with applications of other native starches, the presence of amylose is undesirable. After gelatinization of starch, it forms crystals which reduces the paste clarity. A new type of potato has been bred to solve this problem which contains only amylopectin. It can be developed in two ways. one way consists of treating a mutation-sensitive potato with radiation or chemicals and selecting the desired variety. After successful selection the normal plant cross-fertilization method is applied to produce

potato starch. The second way involves genetic modification of the potato with an antisense technique to eliminate the formation of amylose. The method is less time consuming (10 years) than cross-fertilization program. Amylopectin starches, like waxy maize starch, are mostly used by the food industry. However, amylopectin potato starch has specific properties which are not available in current commercial starches. Native potato starch, which is used in the food, paper and textile industries, is often not optimal for a particular application. Modifications are done to obtain the properties needed for specific uses. More than 500 modifications of potato starch are currently known. Potato starch and its derivatives have special properties, such as a low gelatinization temperature and a high paste consistency. In the paper industry, there is also a preference for potato starch due to the high molecular weight of its amylose and its good solubility. Cationic potato starches are preferred for internal sizing due to the concurrent presence of phosphate groups. Potato starch dextrins also have an advantage over other starches as an adhesive, because of the good remoisten ability [14] and a desirable rheology resulting in a perfect direct tack. Textiles are manufactured better with potato starch due to its film properties, [15] paste penetration depth [16] and adhesive power [17].

1.3 Composite material

Composite is a material combined with two or more constituents of different properties which make significant and unique properties [18]. As an example wood is a natural composite material where long cellulose fiber is matrix and lignin is reinforcement. Composite material has a long history. As early as 3000 B.C. the ancient Egyptians embedded straw in their mud bricks in order to control shrinkage cracks and improve the tensile strength. After that many more new composite materials are invented and scientists are trying to develop its new different properties. A new dimension added in the field of chemistry when the nanomaterials invented. In fiber-reinforced polymer matrix, fiber is reinforcement and polymer is matrix. Reinforcement enhances the strength and stiffness of composites. The best advantage of composite material is that they are light, corrosion resistance as well as strong. Composite materials are becoming more important day by day being used to aerospace [19-21], transportation [22,23], construction [24, 25] sporting goods [26, 27] and marine goods [28-30].

1.4 Nanocomposite materials

A nanocomposite is a multiphase solid material where one of the phases has a nanoscale dimension less than 100 nm [31-32]. Nanocomposites materials are incorporated with nanosized particles into a matrix of standard material. The result of the addition of nanoparticles is drastic improved the properties including mechanical strength, toughness and electrical or thermal conductivity [33]. Usually, nanocomposites are a class of materials in which one or more phases with nanoscale dimensions (0-D, 1- D, and 2-D) are embedded in a metal, ceramic, or polymer matrix.

1.4.1 Polymeric nanocomposite materials

Nanoparticle added as reinforcement into polymer matrix can improve its performance [34]. Nanoparticles such as grapheme, carbon nanotubes are used as reinforcement in polymer matrix as nano-filler for developing the strength and stiffness. Polymer and nanoparticles combinedly give the unique properties due to their mutual interactions. Polymeric nanocomposites are used widely in biomedical applications such as tissue engineering [34], drug delivery system and cellular therapies. Starch [35], cellulose [36], collagen, poly vinyl alcohol (PVA) [37], acrylamide (AAm) [38], acrylic acid (AA) [39] are generally used as polymer matrix.

1.4.2 Application of nanocomposite materials

Nanocomposites materials are currently being used in a number of fields and new applications are being continuously developed. Applications for nanocomposites materials include:

a. Thin-film capacitors for computer chip

b. Solid polymer electrolytes for batteries.

c. Automotive engine parts and fuel tanks

d. Impellers and blades

e. Oxygen and gas barrier

f. Food packaging

g. Drug delivery systems

h. Anti-corrosion barrier coatings

i. UV protective gels

j. Fire retardant materials

k. New scratch/abrasion resistant materials

1.5 Hydrogel

Hydrogels are hydrophilic, highly crosslinked polymeric networks capable of absorbing large amount of water. Hydrogel contains hydrophilic groups such as –OH, -COOH, -NH2, -$CONH_2$ and –SO_3H. It is a polymeric material that exhibits the ability to swell and retain a significant fraction of water within its structure, but will not dissolve in water. They are available in dry or hydrated sheet or gel form. Hydrogel can be stimuli responsive such as pH [40], temperature [41], electric field and magnetic field. These stimuli-sensitive hydrogels can change their swelling behavior of the network structure with changing the external environments. Temperature sensitive hydrogels are known as thermogels. Hydrogels are generally highly biocompatible, which may be attributed due to the presence of high water content in the network. Cross-linking can render these gels insoluble and provide additional mechanical strength. Such gels swell by imbibing small to large quantities of water. Hydrogels are generally synthesized by free radical polymerization of the monomer. The ability of hydrogels to absorb water arises from hydrophilic functional groups attached to the polymeric backbone, while their resistance to dissolution arises from cross-links between network chains. Many materials, both naturally occurring and synthetic, fit the definition of hydrogels.

1.5.1 Hydrogels and their properties

Back to 1960, the pioneering work of Wichterle and Lim introduced hydrophilic hydrogels for biological uses [42]. During the past decades, hydrogels have gained tremendous interest to the scientist due to their exceptional promise in biomaterial applications. More than 50,000 reports have been published on hydrogel up to now. Hydrogel exists in nature since the evolution of life. Bacterial biofilms, hydrated living tissues and extracellular matrix components are some examples. A variety of naturally occurring polymers such as collagen, alginate, agarose and gelatin were also explored in early human history. However the modern history of hydrogels as a class of materials designed for medical uses. Dates back to the late 1950s, Poly (2-hydroxyethyl methacrylate) commonly known as PHEMA was the synthetic hydrogel to be synthesized in 1936 by DuPont Scientist, but it was not until 1960 that Wichterle and Lim established the importance of PHEMA hydrogels as excellent candidates for contact lens applications. This success generated

enormous interest in hydrogels and led to the development of smart hydrogels that can change their properties of an external stimulus such pH, temperature, magnetic field, ionic strength or electric field. Hydrogels began to be expanded in various research fields such as biomaterials, agriculture, pharmaceuticals and biotechnology. More recently hydrogels have become especially attractive to the field of tissue engineering as matrices for repairing and regenerating a widely of tissues and organs. Hydrogels have a variety of properties including their absorption capacity, swelling behavior, permeability, surface properties, optical properties and mechanical properties which make them promising materials for manifold applications. The characteristics of the polymer chains and the crosslinking structures play a vital role in the outcome of the properties of hydrogels.

1.6 Mechanical properties of hydrogels

The mechanical properties of hydrogels depend on their composition and structure. Because of the high water content of fully swollen hydrogels, they normally have weak mechanical strengths. The mechanical properties of the hydrogel are affected by the co-monomer composition, crosslinking density, polymerization conditions and degree of swelling. The mechanical strength of the hydrogel is often derived entirely from the crosslinks in the system, particularly in the swollen state where physical entanglements are almost nonexistent. The dependence of mechanical properties on crosslink density has been studied intensively by many researchers. However it should be noted that when the crosslinking density is altered, change in properties rather than strength also occur. For example, increasing the crosslinker concentration would make the polymer chains to come closer, thus reducing the diffusivity, release and swelling rates including the maximum degree of swelling. These properties should be re-measured every time whenever additional crosslinks are added.

The mechanical behavior of hydrogels is best understood by theories of elasticity and viscoelasticity. These theories are based on the time-independent and time-dependent recovery of the chain orientation and structure respectively. Elasticity theory assumes that when a stress is applied to the hydrogel the strain response is instantaneous. However for many biomaterials, including hydrogels and tissues, this is not a valid assumption. For example, if a weight is suspended from a specimen of ligament, the ligament continues to extend even though load is constant. Similarly, if the ligament is elongated to a fixed

length, the load will drop continuously with time. This is due to creep and stress relaxation, respectively and these result viscous flow in the material.

Mechanical properties of hydrogels are also very important from the pharmaceutical and biomedical point of view. The evaluation of mechanical property is essential in various biomedical applications viz. ligament and tendon repair, wound dressing material, matrix for drug delivery, tissue engineering and as cartilage replacement material. The mechanical properties of hydrogels should be such that it can maintain its physical texture during the delivery of therapeutic moieties for the predetermined period of time. Changing the degree of cross-linking, the desired mechanical property of the hydrogel could be achieved. By increasing the degree of cross-linking, a stronger hydrogel could be achieved through the higher degree of cross-linking but simultaneously it decreases the percent of elongation of the hydrogels and creates a more brittle structure. Hence, there is an optimum degree of cross-linking to achieve a relatively strong and yet elastic hydrogel. Copolymerization with co-monomer, may result into hydrogen bonding within the hydrogel which has also been utilized by many researchers to achieve desired mechanical properties.

1.6.1 Tensile strength

The maximum stress that a material can withstand while being stretched or pulled before failing or breaking is known as Tensile strength. Elongation at break, also known as fracture strain, is the ratio between changed length and initial length after breakage of the test specimen. On the other hand, stress is defined as force per unit area. It has the same units as pressure, and in fact pressure is one special variety of stress. However, stress is a much more complex quantity than pressure because it varies both with direction and active surface. Strain is defined as the amount of deformation an object experiences compared to its original size and shape.

1.6.2 Stress-Strain diagram

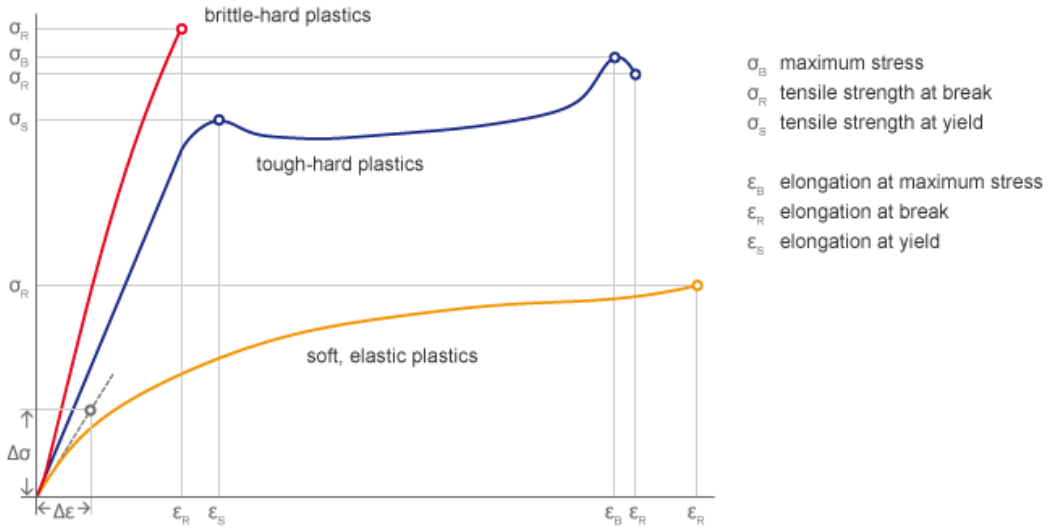

Figure 1.4: Typical stress-strain curve of materials

The tensile strength of a material quantifies how much stress the material will endure before failing [43] .This is very important in applications that rely upon polymer's physical strength or durability. For example, a rubber band with a higher tensile strength will hold a greater weight before snapping. Usually tensile strength increases with polymer chain length in the polymer matrix.

1.6.3 Young's modulus of elasticity

Young's Modulus quantifies the elasticity of the polymeric materials. It is defined as the ratio of rate of change of stress to strain. Like tensile strength, this is highly relevant in polymer applications involving the physical properties of polymers. It indicates the elastic region of the materials without experiencing any deformation of the materials.

1.7 Biodegradability and surface properties of hydrogels

Biocompatibility is the ability of a hydrogel to reside in the body without inducing significant immune response or toxicity. The important question in biocompatibility is how the hydrogel transduces its structural makeup to direct or influence the response of proteins, cells and organisms. This transduction occurs through the surface properties of the hydrogel, i.e. the body reads the surface structure and responds to it. The surface of a hydrogel can be rough, smooth or stepped; it can be composed of different chemistries or could be highly crystalline, disordered and inhomogeneous. Studies have been performed

on the importance of roughness, wettability, surface mobility, chemical composition, crystallinity and heterogeneity, however significant research has not yet been performed on determining which parameters are of utmost importance in understanding biological responses to surfaces. Some of the techniques used for determining the surface property include electron spectroscopy [44], scanning electron microscopy, fourier transform infrared spectroscopy [45], scanning tunneling microscopy and atomic force microscopy. The information obtained using these methods can be used to monitor contamination, ensure surface reproducibility and explore the interaction of the hydrogels with living systems.

1.7.1 Permeability of hydrogels

Permeability is the ability of a hydrogel to transmit another substance such as fluids, cells or proteins. Developing hydrogel membranes and coatings of appropriate permeability characteristics is key to the success of a number of bioartificial organ transplantations. The permeability of a hydrogel to water and solutes can be adjusted over a wide range by varying the crosslinker concentration at synthesis or copolymerizing with more hydrophilic or hydrophobic monomers. Some of the real life situations where permeability of hydrogels is critical are oxygen permeation for contact lens applications, nutrient and immunological biosubstance transport for immune isolation and release of drugs and proteins for drug delivery systems.

1.7.2 Stimuli responsive hydrogels

Responsive hydrogels are called smart or intelligent hydrogel. After the discovery of responsive hydrogels in the late seventies by Tanaka large numbers of polymers were identified, responding to all thinkable stimuli. Hydrogels usually response to changes in temperature, pH, pressure, electric field, magnetic field, chemical stimuli, light and to irradiation. Small changes can show more significant result. The application and development of temperature-responsive and pH-responsive system have been extensively studied for stimuli – responsive drug delivery.

1.7.3 pH responsive hydrogel

Response to pH is widely found stimulus, which originates from the electrostatic repulsion between charged groups within the polymer. At high pH polyacrylates show enhanced swelling, whereas polyamines exhibit the same behavior at low pH.

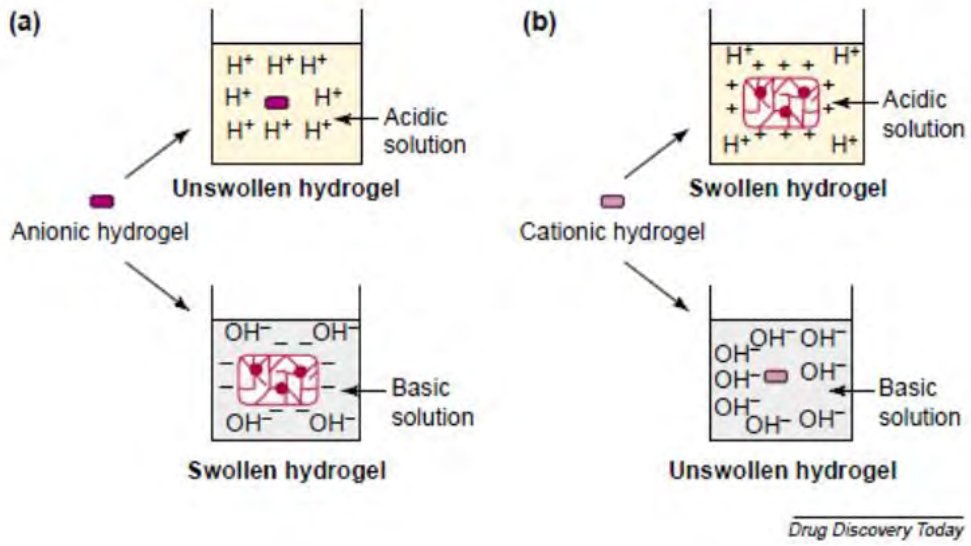

Figure 1.5: The pH-responsive swelling of (a) anionic and (b) cationic hydrogels

1.7.4. Temperature responsive hydrogel

Another important stimulus for causing hydrogel responsiveness is temperature. Polymers, which become insoluble upon heating, have a so-called lower critical solution temperature (LCST). Systems, which become soluble upon heating, have an upper critical solution temperature (UCST). Some hydrogels are temperature sensitive as they exhibit a critical solution temperature. Most of them show a decreased solubility in water with rising temperature. Above their lower critical solution temperature, they collapse. Interestingly, the opposite behavior also exists as well. Few polymers are known to have an upper critical temperature. Temperature sensitive polymers are generally pressure sensitive as well.

1.8 Applications of hydrogels:

Common applications of hydrogels include:

 Scaffolds in tissue engineering. When used as scaffolds, hydrogels may contain human cells to repair tissue. They mimic 3D microenvironment of cells [46].

 Hydrogel-coated wells have been used for cell culture [47].

 Environmentally sensitive hydrogels (also known as 'Smart Gels' or 'Intelligent Gels') have the ability to sense changes of pH, temperature, or the concentration of metabolite and release their load as result of such a change [48].

 Sustained-release drug delivery systems.

 Providing absorption, desloughing and debriding of necrotic and fibrotic tissue

 Hydrogels that are responsive to specific molecules, such as glucose or antigens, can be used as biosensors, as well as in DDS [49].

 Disposable diapers where they absorb urine, or in sanitary napkins [50].

 Contact lenses (silicone hydrogels, polyacrylamides, polymacon).

 EEG and ECG medical electrodes using hydrogels composed of crosslinked polymers (polyethylene oxide, polyAMPS and polyvinylpyrrolidone).

 Water gel explosives.

 Encapsulation of quantum dots.

 Breast implants.

 Granules for holding soil moisture in arid areas.

 Dressings for healing of burn or other hard-to-heal wounds. Wound gels are excellent for helping to create or maintain a moist environment.

 Reservoirs in topical drug delivery; particularly ionic drugs, delivered by iontophoresis (see ion exchange resin).

 Materials mimicking animal mucosal tissues to be used for testing mucoadhesive properties of drug delivery systems [51].

1.9 Cross-linker

Cross-linking is the process of chemically joining two or more molecules or polymer chains by a covalent bond. Generally, which agents perform this joining work is called cross-linker. Cross-linkers contain at least two reactive groups. Reactive groups that can be targeted for crosslinking include primary amines, sulfhydryl‟s, carbonyls, vinyl group, carbohydrates, carboxylic acids etc. When polymer chains are linked together by cross-linker, they lose some of their ability to move as individual polymer chains. Hence

chemical crosslinking are mechanically and thermally stable. Cross-linking may be initiated by heat, pressure, change in pH, or radiation. Cross-linkers are chosen depending on chemical specificity, same or different reactive groups, spontaneously reactive or photoreactive groups etc. They are commonly used to modify nucleic acids, drugs and solid surfaces.

1.9.1 Significance of Cross-linking

Water-logged gels of crosslinked polyacrylamides are used to make soft contact lenses. Adding cross-links between polymer chains affect the physical properties of the polymer depending upon the degree of cross-linking and presence and absence of crystallinity. Cross-linking results in:

i) **Elasticity:** Elastomers are elastic polymers created by limited cross-linking. As the number of cross-links increases, however, the polymer becomes more rigid and cannot stretch as much; the polymer will become less viscous and less elastic and might even become brittle. The vulcanization or sulfur curing of rubber, for example, results from the introduction of short chains of sulfur atoms that link the polymer chains in natural rubber. Bridges made by short chains of sulfur atoms tie one chain of polyisoprene to another, until all the chains are joined into one giant super molecule. The chemical process of vulcanization is a type of cross-linking which increases the strength of rubber. It makes rubber hard and durable material associated with car and bike tires.

ii) **Decrease in the viscosity:** The resistance to flow of polymers is realized from decrease in the viscosity . In order to flow of polymers, the chains must move past each other and cross-linking prevents this. As a result of restriction in flow, there is improvement in the creep behavior.

iii) **Insolubility of the polymer:** Cross-linking results in insolubility as the chains are tied together by strong covalent bonds. Cross-linked materials can't dissolve in solvents, but can absorb solvents to form a *gel*. Uncrosslinked polyacrylamide is soluble in water but cross-linked polyacrylamides chains can absorb water to produce hydrogel.

iv) **Increased Tg and increase strength and toughness**: Cross-linking changes the local molecular packing, resulting decrease in free volume, leading to increase in Tg. PVA cross-linked with boric acid shows increased glass transition temperature [52]. Cross-links slow down the PVA molecular motion and must not be included in the crystalline domains.

v) **Lower melting point**: For crystalline polymer with low degree of cross-linking there is a decrease in the crystalline behavior. As cross-linking introduces hindrance to the chain orientation resulting in softer, elastic polymer having lower melting point.

vi) **Transformation of therrmoplastics into thermosets**: Heavy cross-linking changes therrmoplastics to thermoset plastics. Once the cross-links form, the polymer‟s shape cannot be changed again without destroying the plastic. Unlike thermoplastic polymers, the process cannot be undone by reheating. Thermoset plastics will start to decompose rather than becoming moldable and pliable. The first reported thermoset is polyisoprene. More the sulfur crosslinks put into the polyisoprene, the stiffer it gets. Lightly cross-linked gives a flexible rubber but heavily crosslinked gives a hard thermoset.

1.9.2 Hydrogels and Crosslinking

The term "hydrogel" represent water insoluble polymeric network that has capacity to absorb large amount of water [53-57]. A hydrogel is a macromolecular polymer gel constructed of a network of cross-linked polymer chains. They are synthesized from hydrophlic monomers by either chain or step growth polymerizations in presence of a functional crosslinker to promote network formation. Synthetic or natural polymers, homopolymer or copolymer, are used to make three dimensional networks by molecular entanglements or by chemical cross-linking [58].

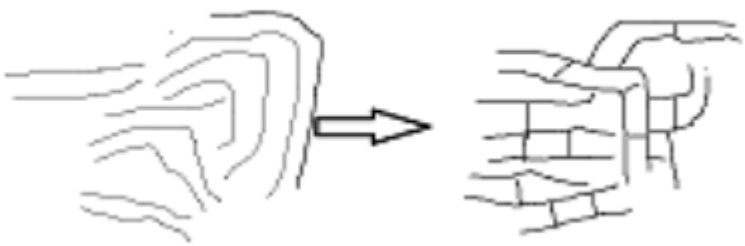

Figure 1.6: Cross-linking in polymer

The property of hydrogels to swell under biological conditions makes them an ideal class of materials for biomedical applications, such as drug delivery system and tissue engineering [59] [60]. Cross-linking either physically or chemically gives hydrogel a 3D network structure, making it insoluble and allows effective immobilization and release of active agents and biomolecules. Hydrogels appear similar to natural soft tissues because of their high water content.

Table 1.1: The name of some typical hydrogels, their cross-linking agents and applications.

Hydrogel	Cross linking agent	Applications
Poly Vinyl Alcohol	Sodium borate/ boric acid [52]	Packaging
Polyvinyl alcohol	Glyoxal	Adhesives Plastic films for packaging and water-soluble plastic bags Binders Fuel-resistant hoses Starch
Starch	Glyoxal	Paper industry
Cellulose	Glyoxal	Textile industry
Protein and gelatin	Glyoxal	Food packaging
Polyethylene	Silane	Wires, cables, pipes heat shrinkable tubes
Agarose and chitosan	Oxidized dextrins [73]	Tissue engineering
Chitosan	Glutarldehyde [74]	Scaffold of hepatocyte
Guar gum	Epichlorohydrin [75]	Biomedical field
Gellan gum	Endogen polyamine spermidine [76]	Drug delivery
Glycol chitosan	Oxidized alginate [77]	Drug delivery
Hydroxamated alginates	Zinc [78]	Drug delivery
Alignate bead	Zinc [79]	Drug delivery
Scleroglucan	Borax[80]	Drug delivery
Poly(acrylic-co-vinylsulfonic) acid	Ethylene glycol dimethacrylate (EGDMA) [81]	Drug delivery
Polyacrylamide	N,N′-methylenebisacrylamide [82]	Dehydrating agent
Polyacrylamide/guar gum graft copolymer	Glutaraldehyde [83]	Sorbent material for chromium ion (Cr (VI)
Polyacrylamide/guar gum graft copolymer	Glutaraldehyde [84]	Water transport and drug release

1.10 Literature Review:

Hydrogel, a three-dimensional network of hydrophilic polymers, can swell in water and hold a large amount of water while maintaining its structure. It is formed by cross-linking of polymer chains by covalent bonds, hydrogen bonds, vander Waals interactions and physical entanglements. Due to its unique properties, hydrogel was applied in drug delivery system, biomedical and tissue engineering etc [85-87]. However most of the hydrogels suffer from a lack of mechanical performance. The poor mechanical property of hydrogel has often limited its further industrial and biomedical applications [88-89]. Recently, a lot of research work has been devoted to improve the mechanical performance of hydrogel [90-91]. Different hydrogels are considered to be a simple way of improving the mechanical properties of hydrogels with the use of different cross-linker. Desired mechanical property of the hydrogel could be achieved by changing the degree of cross-linking. A strong hydrogel could be achieved through the higher degree of cross-linking which decreases the elongation of the hydrogels creates a more brittle structure. For the purpose of different applications, hydrogel is synthesized using different types of cross-linker. But most of the cross-linkers are not biodegradable and non-toxic. Therefore, it has been attempted to synthesize a biodegradable cross-linker which is not detrimental for nature and human body. Starch based nano composite has extraordinary characteristics. It has also primary and secondary hydroxyl group and these groups can easily be modified to fabricate cross-linker. In the proposed research, the core aim is to fabricate a cross-linked polymer composite where modified nano starch will be employed as a cross-linker. It is well-established that the cross-linked polymers using traditional cross-linkers show enhanced mechanical properties, but the increase of cross-linker density in polymer networks may lead to immobilization of molecular chain, hardness and brittleness which limits the fields of their applications. Therefore, modified nano-starch cross-linker as described in the proposal are expected to overcome the drawbacks of the traditionally cross-liked hydrogels.

1.10.1 The aim of the Current Research

The aims of this research were the following:

- to synthesis biodegradable nano-starch from microcrystalline starch
- to incorporate active vinyl groups into nano-starch to have cross-linker
- to synthesis a mechanically strong hydrogel using biodegradable nano-starch cross-linker and
- to ensure high mechanical properties of this synthesized hydrogel.

References

[1] Hizukuri, S., Takeda, Y., Maruta, N., Juliano, B. O., "Molecular structures of rice starch," *Carbohydrate Research,* Vol. 227, pp. 189, 1989.

[2] Takeda, Y., Hizukuri, S., Takeda, C., Suzuki, A., "Structures of branched molecules of amyloses of various origins, and molar fractions of branched and unbranched molecules," *Carbohydrate Research*, Vol. 139, pp. 165, 1987.

[3] Hizukuri, S., Takeda, Y., Yasuda, M. and Suzuki, A., "Multi-branched nature of amylose and the action of debranching enzymes," *Carbohydrate Research*, Vol. 94, pp. 205, 1981.

[4] Imberty, A., Chanzy, H., Perez, S., Buleon, A., and Tran, V., "The double-helical nature of the crystalline part of A-starch," *Molecular Biology,* Vol. 201, pp. 365, 1988.

[5] Pervez, S., Aman, A., Iqbal, S., et al., "Saccharification and liquefaction of cassava starch: an alternative source for the production of bioethanol using amylolytic enzymes by double fermentation process," *BMC Biotechnol.*, Vol. 14(49), 2014.

[6] Szejtli, J. J., *Inclusion Phenom,* Vol. 11, pp. 135, 1983.

[7] Hirai, S., Okada, H., and Yashiki, T., *US Patent,* Vol. 4 , pp. 659-696, 1987.

[8] Pomeranz, Y., "Wheat Chemistry and Technology," American Association of Cereal Chemists, 3rd edn., Chapt. 6, Vol. II, pp. 514, 1988.

[9] Lineback, D., Rasper, V., "Wheat Chemistry and Technology," American Association of Cereal Chemists, 3rd edn., Chapt. 4, Vol. I, pp. 562, 1988.

[10] Simmonds, N. W., "The Relation Between Yield and Protein in Cereal Grain", *J. Sci. Food Agric.,*Vol. 67, pp. 309-315, 1995.

[11] Gardlick, J. M., Trinh, T., Barks, T. J., Benvegnu, F., *US Patent*, Vol. 5, pp. 234,610, 1993.

[12] Trinh, T., Bacon, D. R., Benvegnu, F., *US Patent,* Vol. 5, pp. 234, 1993.

[13] Wiedenhof, N., Lammers, J. N. J. J., *Carbohydr. Res*., Vol. 1, pp. 7, 1968.

[14] Vakaliu, H., Miskolczi-Torak, M., Szejtli, J., Jarai, M., Seres, G., *Hungarian Patent,* Vol. 16, pp. 98, 1979.

[15] Shieh, W. J., Hedges, A. R., US *Patent,* Vol. 5, pp. 326, 1994.

[16] Schmidt, G., Duchene, D., “New Trends in Cyclodextrins and Derivatives,” pp. 25, 1991.

[17] Wiedenhof, N., Lammers, J. N. J. J., *Carbohydr. Res.,* Vol. 1, pp. 7, 1968.

[18] Ahmed, E.M., *Hydrogel: "*Preparation, characterization, and applications*:* A review*," Journal of Advanced Research*, Vol. 6(2), pp. 105-121, 2015.

[19] Armentano, I., "Biodegradable polymer matrix nanocomposites for tissue bengineering: a review," *Polymer degradation and stability*, Vol. 95(11), pp. 2126-2146, 2010.

[20] Armentano, I., "Biodegradable polymer matrix nanocomposites for tissue engineering: a review", *Polymer degradation and stability*, Vol. 95(11), pp. 2126-2146, 2010.

[21] Bajpai, A. and Giri, A., "Water adsorption behaviour of highly swelling (carboxy methylcellulose- g-polyacrylamide) hydrogels and release of potassium nitrate as agrochemical," *Carbohydrate polymers*, Vol. 53(3), pp. 271-279, 2003.

[22] Bekyarova, E., et al., "Multiscale carbon nanotube- carbon fiber reinforcement for advanced epoxy composites,” *Langmuir,* Vol. 23(7), pp. 3970-3974, 2007.

[23] Bleay, S., et al., “A smart repair system for polymer matrix composites,” *Composites Part A: Applied Science and Manufacturing,* Vol. 32(12), pp. 1767-1776, 2001.

[24] Brannon-Peppas, L., and Peppas, N. A., “Dynamic and equilibrium swelling behaviour of pH sensitive hydrogels containing 2-hydroxyethyl methacrylate,” *Biomaterials,* Vol. 11(9), pp. 635-644, 1990.

[25] Chawla, K. K., "Ceramic matrix composites, in Composite Materials," *Springer.* pp. 212-251. 1998.

[26] Day, J. W., et al., “Restoration of the Mississippi Delta: lessons from hurricanes Katrina and Rita,” *science,* Vol. 315(5819), pp. 1679-1684, 2007.

[27] Day, J.W., et al., Restoration of the Mississippi Delta: lessons from hurricanes Katrina and Rita”, *science,* Vol. 315(5819), pp. 1679-1684, 2007.

[28] Devasahayam, S., Bandyopadhyay, S., and Hill, D. J., "Study of Victorian Brown Coal Dewatering by Super Absorbent Polymers using Attenuated Total Reflection Fourier Transform Infrared Spectroscopy," *Mineral Processing and Extractive Metallurgy Review*, Vol. 37(4), pp. 220-226, 2016.

[29] Dokos, L., "Adoption of marine composites–a global perspective" *Reinforced Plastics,*" Vol. 57(3), pp. 30-32, 2013.

[30] Ferfera-Harrar, H., Aouaz, N., and Dairi, N., "Environmental-sensitive chitosan gpolyacrylamide/ carboxymethylcellulose superabsorbent composites for wastewater purification I: synthesis and properties*," Polymer Bulletin,* Vol. 73(3), pp. 815-840. 2016.

[31] Giannelis, E. P., "Polymer layered silicate nanocomposites", *Advanced materials,* Vol. 8(1), pp. 29-35, 1996.

[32] Giannelis, E. P., "Polymer layered silicate nanocomposites," *Advanced materials*, Vol. 8(1), pp. 29-35 1996.

[33] Gupta, P., Vermani, K., and Garg, S., "Hydrogels: from controlled release to pH-responsive drug delivery," *Drug discovery today*, Vol. 7(10), pp. 569-579, 2002.

[34] Hamidi, M., Azadi, A., and Rafiei, P., "Hydrogel nanoparticles in drug delivery" *Advanced Drug Delivery Reviews,* Vol. 60(15), pp. 1638-1649, 2008.

[35] Horn, M. M., Martins, V. C., and GuzziPlepis, A. M., "Influence of collagen addition on the thermal and morphological properties of chitosan/xanthan hydrogels," *International Journal of Biological Macromolecules*, Vol. 80, pp. 225-230, 2015.

[36] Ishigaki, I., et al., "Graft polymerization of acrylic acid onto polyethylene film by preirradiation method. II. Effects of preirradiation dose, monomer concentration, reaction temperature, and film thickness," *Journal of Applied Polymer Science*, Vol. 27(3), pp. 1033-1041, 1982.

[37] Kabiri, K., et al., "Synthesis of fast-swelling superabsorbent hydrogels: effect of crosslinker type and concentration on porosity and absorption rate," *European Polymer Journal*, Vol. 39(7), pp. 1341-1348, 2003.

[38] Kaczmar, J., Pietrzak, K., and Włosiński, W., "The production and application of metal matrix composite materials," *Journal of Materials Processing Technology,* Vol. 106(1), pp. 58-67, 2000.

[39] Kok, M., "Production and mechanical properties of Al_2O_3 particle-reinforced 2024 aluminium alloy composites," *Journal of Materials Processing Technology,* Vol. 161(3), pp. 381-387, 2005.

[40] Hongbo, T., Yanping, L., Min, S., et al., "Preparation and property of crosslinking guar gum," *Polym., J.*, Vol. 44, pp. 211-216, 2012.

[41] Yokoyama, F., Masada, I., Shimamura K., et al., "Morphology and structure of highly elastic poly(vinyl alcohol) hydrogel prepared by repeated freezing-andmelting," *Colloid and Polymer Science,* Vol. 264, pp. 595-601, 1986.

[42] Devasahayam, S., Bandyopadhyay, S., and Hill, D. J., "Study of Victorian Brown Coal Dewatering by Super Absorbent Polymers using Attenuated Total Reflection Fourier Transform Infrared Spectroscopy," *Mineral Processing and Extractive Metallurgy Review*, Vol. 37(4), pp. 220-226, 2016.

[43] Veis, A., Horecker, B., Kaplan, N. O., Scheraga, H. A., "In The Macromolecular Chemistry of Gelatin," *Academic: New York,* 5, 1964.

[44] Ferfera-Harrar, H., Aouaz, N., and Dairi, N., "Environmental-sensitive chitosan gpolyacrylamide/carboxymethylcellulose superabsorbent composites for waste water purification I: synthesis and properties," *Polymer Bulletin*, Vol. 73(3), pp. 815-840, 2016.

[45] Wichterle, O., and Lim, D,. "Hydrophilic Gels for Biological *Use," Nature,* Vol. 185 (4706), pp. 117-118, 1960.

[46] Mellati, A., Dai, S., Bi, J., et al., "A biodegradable thermosensitive hydrogel with tuneable properties for mimicking three-dimensional microenvironments of stem cells," *RSC Advances,* Vol. 4, pp. 63951-63961, 2014.

[47] Discher, D. E., Janmey, P., and Wang, Y., "Tissue Cells Feel and Respond to the Stiffness of Their Substrate," *Science,* Vol. 310, pp. 1139-1143, 2005.

[48] Brudno, Y., and Mooney, D. J., "On-demand drug delivery from local depots*," Journal of Controlled Release,* Vol. 219, pp. 8-17, 2015.

[49] Yetisen, A. K., Naydenova, I., Vasconcellos, F. D. C., et al., "Holographic Sensors: Three-Dimensional Analyte-Sensitive Nanostructures and Their Applications," *Chemical Reviews,* Vol. 114, pp. 10654-10696, 2014.

[50] Caló, E., and Khutoryanskiy, V. V., "Biomedical applications of hydrogels: A review of patents and commercial products," *European Polymer Journal*, Vol. 65, pp. 252-267, 2015.

[51] Cook, M. T., Smith, S. L., and Khutoryanskiy, V., "Novel glycopolymer hydrogels as mucosa-mimetic materials to reduce animal testing," *Chemical Communications*, Vol. 51, pp. 14447-14450, 2015.

[52] Tsukasa, M., Yuuki, T., Sachiko, A., Takahiko, I., Akie, H., Keiko, E., "Role of boric acid for a poly (vinyl alcohol) film as a cross-linking agent: Melting behaviors of the films with boric acid", *Polymer,* Vol. 51, pp. 5539–5549, 2010.

[53] Nguyen, K., T., West, J. L., "Photopolymerizable hydrogels for tissue engineering applications," *Biomaterial,* Vol. 23, pp. 4307- 4314, 2002.

[54] Peppas, N. A., Bures, P., Leobandung, W., Ichikawa, H., "Hydrogels in pharmaceutical formulations" *Eur. J. Pharm. Biopharm*," Vol. 50, pp. 27-46, 2000.

[55] Sawhney, A. S., Pathak, C. P., Rensburg J. J. V., Dunn R., C., Hubbell J. A., "Optimization of photopolymerized bioerodible hydrogel properties for adhesion prevention," *Journal of Biomedical Materials Research,* Vol. 28, pp. 831-838, 1994.

[56] Kopecek, J., "Hydrogel biomaterials: a smart future?" *Biomaterials,* Vol. 28(34), pp. 5185–5192, 2007.

[57] Lutolf, M. P., "Biomaterials: Spotlight on hydrogels," *Nat Materials*, Vol. 8(6), pp. 451–453, 2009.

[58] Chung, H. K., Park, T. G., "Self-assembled and nanostructured hydrogels for drug delivery and tissue engineering," *NanoToday*, Vol. 4(5), pp. 429–437, 2009

[59] Oh, J. K., "Engineering of nanometer-sized cross-linked hydrogels for biomedical applications," *Can J Chem*, Vol. 88(3), pp. 173–184, 2010.

[60] Ulijn, R. V., Bibi, N., Jayawarna, V., et al., "Bioresponsive hydrogels," *Mater Today,* Vol. 10(4), pp. 40–48. 2007.

[61] Lee, J., Cuddihy, M. J., Kotov, N. A., "Three-dimensional cell culture matrices: state of the art," *Tissue Eng Part B*, Vol. 14(1), pp. 61–86, 2008.

[62] Geckil, H., Xu, F., Zhang, X. H., Moon, S., Demirici, U., "Engineering hydrogels as extracellular matrix mimics, *Nanomedicine,* Vol. 5(3), pp. 469–484, 2010.

[63] Hunt, N. C., Grover, L. M., "Cell encapsulation using biopolymer gels for regenerative medicine," *Biotechnol. Lett.,* Vol. 32(6), pp. 733–742, 2010.

[64] Drury, J. L., Mooney, D. J., "Hydrogels for tissue engineering: scaffold design variables and applications," *Biomaterials*, Vol. 24(24), pp. 4337–4351, 2003.

[65] Liu, S. Q., Tay, R., Khan, M., Ee, P. L. R., Hedrick, J. L., Yang, Y. Y., Synthetic hydrogels for controlled stem cell differentiation," *Soft Matter*, Vol. 6(1), pp. 67–81, 2010.

[66] Slaughter, B. V., Khurshid, S. S., Fisher, O. Z., Khademhosseini, A., Peppas, N. A., "Hydrogels in regenerative medicine," *Adv. Mater,* Vol. 21(32–33), pp. 3307–3329, 2009.

[67] Nicodemus, G. D., Bryant, S. J., "Cell encapsulation in biodegradable hydrogels for tissue engineering applications," *Tissue Eng. Part B Rev.*, Vol. 14(2), pp. 149–165, 2008.

[68] Cushing, M. C., Anseth, K. S., "Hydrogel cell culture," *Science*, Vol. 316(5828), pp. 1133–1134, 2007.

[69] Miyata, T., Uragami, T., Nakamae, K., "Biomolecule-sensitive hydrogels," *Adv. Drug Deliv. Rev.,* Vol. 54, pp. 79-98, 2002.

[70] Chang, C., Duan, B., Cai J., Zhang, L., "Superabsorbent hydrogels based on cellulose for smart swelling and controllable delivery," *Eur. Polym. J.,* Vol. 21, pp. 92–100, 2010.

[71] Nguyen, T. K., West, J. L., "Photopolymerizable hydrogels for tissue engineering applications," *Biomaterials,* Vol. 23(22), pp. 4307–4314, 2002.

[72] Aly, A. S., "Self-dissolving chitosan. I. Preparation and characterisation and evaluation for drug delivery system," *Angew. Macromolecular Chemistry*," Vol. 259, pp. 33-38. 1998.

[73] Gómez-Mascaraque, L. G., Méndez, J. A., Fernández-Gutiérrez M., Vázquez B., San Román J., "Oxidized dextrins as alternative crosslinking agents for

polysaccharides: application to hydrogels of agarose-chitosan," *Acta. Biomater.,* Vol. 10(2), pp.798-811, 2014.

[74] Kawase, M., Michibayashi, N., Nakashima, Y., Kurikawa, N., Yagi, K., Mizoguchi, T., "Application of glutaraldehyde-crosslinked chitosan as a scaffold for hepatocyte attachment," *Biol. Pharm. Bull*., Vol. 20(6), pp. 708-710, 1997.

[75] Hongbo, T., Yanping, L., Min, S., and Xiguang, W., "Preparation and property of crosslinking guar gum," *Polymer Journal*, Vol. 44, pp. 211–216, 2012.

[76] López-Cebral, R., Paolicelli, P., Romero-Caamaño, V., Seijo, B., Casadei, M. A., "Sanchez Aspermidine-cross-linked hydrogels as novel potential platforms for pharmaceutical applications," *J. Pharm. Sci*., Vol. 102(8), pp. 2632-43, 2013.

[77] Xu, X., Weng, Y., Xu, L., Chen, H., "Sustained release of avastin® from polysaccharides cross-linked hydrogels for ocular drug delivery," *International Journal of Biological Macromolecules*, Vol. 60, pp. 272–276, 2013.

[78] Raut, N. S., Deshmukh, P. R., Umekar, M. J., Kotagale, N. R., "Zinc cross-linked hydroxamated alginates for pulsed drug release", *Int. J. Pharm. Investig.*, Vol. 3(4), pp. 194-202, 2013.

[79] Taha, M. O., Nasser, W., Ardakani, A., Alkhatib, H. S., "Sodium lauryl sulfate impedes drug release from zinc-crosslinked alginate beads: switching from enteric coating release into biphasic profiles," *Int. J. Pharm.*, Vol. 28, pp, 350(1-2): 291-300, 2008.

[80] Coviello, T., Grassi, M., Lapasin, R., Marino, A., Alhaique, F., "Scleroglucan/borax: characterization of a novel hydrogel system suitable for drug delivery," *Biomaterials,* Vol. 24(16), pp. 2789-98, 2003.

[81] Hussain, T., Ansari, M., Ranjha, N. M., Khan, I. U., Shahzad, Y., "Chemically cross-linked poly(acrylic-co-vinylsulfonic) acid hydrogel for the delivery of isosorbidemononitrate," *Scientific World Journal,* Vol. 23, pp. 01-09, 2013.

[82] Sherr, A. E., and Swift A. M., "Crosslinked polyacrylamide gel as a dehydrating agent," *Journal of Applied Polymer Science",* Vol. 99(12), pp. 3929–3934, 1965.

[83] Abdel-Halim,E. S., Al-Deyab, S. S., "Hydrogel from cross-linked polyacrylamide/guar gum graft copolymer for sorption of hexavalent chromium ion", *Carbohydrate Polymers,* Vol. 86, pp. 1306–1312, 2011.

[84] Soppirnath, K. S., Aminabhavi, T. M., "Water transport and drug release study from cross-linked polyacrylamide grafted guar gum hydrogel microspheres for the controlled release application," *Eur. J. Pharm. Biopharm.*, Vol. 53(1), pp. 87-98, 2002.

[85] Hoffman, A. S., "Hydrogels for biomedical applications,"" *Adv. Drug Delivery Rev.*, Vol. 64, pp. 18-23, 2012.

[86] Qiu, Y., Park, K., "Environment sensitive hydrogels for drug delivery," *Adv. Drug Delivery* Rev., Vol. 53(3), pp. 321-339, 2001.

[87] Kloxin, A. M., Kasko, A. M., Salinas, C. N., and Anseth, K. S., "Photodegradable hydrogels for dynamic tuning of physical and chemical properties," *Science,* Vol. 324, pp. 59-63, 2009.

[88] Itagaki, H., Kurokawa, T., Furukawa, H., Nakajima, T., Katsumoto, Y., Gong, J. P., "Water- induced brittle-ductile transition of double network hydrogels," *Macromolecules,* Vol. 43, pp. 9495-9500, 2010.

[89] Nakajima, T., Furukawa, H., Tanaka, Y., Kurokawa, T., Osada, Y., and Gong, J. P.,"True chemical structure of double network hydrogels," *Macromolecules,* Vol. 42(6) pp. 2184-2189, 2009.

[90] Nakayama, A., Kakugo, A., Gong, J. P., Osada, Y., Takai, M., Erata, T., and Kawano, S., "High mechanical strength double-network hydrogel with bacterial cellulose," Adv. Funct. Mater., Vol. 14, pp. 1124-1128, 2004.

[91] Tanaka, Y., Gong, J. P., and Oasda, Y., "Novel hydrogels with excellent mechanical performance," *Prog. Polym. Sci.,* Vol. 30(1), pp. 1-9, 2005.

Chapter 2

Experimental

2.1 Materials and instruments

2.1.1 Chemicals and reagents

All chemicals and reagents used in this research were analytical grade and used without further purification. Deionized water was used as solvent to prepare most of the solutions of this work. The chemicals and reagents which were used in this research are given below:Micro starch powder (Scharlab, Spain)

- Sulfuric acid (RCI, Lab Scan)
- Sodium hypochlorite (Merck, Germany)
- Sodium bromide (Loba, India)
- 2,2,6,6-tetramethylpiperidine-1-oxyl (TEMPO) (Sigma Aldrich)
- Ethanol (Merck, Germany)
- Sodium hydroxide (Merck, Germany)
- Sodium chloride (Merck, India)
- Potassium chloride (Merck, India)
- Sodium hydrogen phosphate(Merck, India)
- Potassium dihydrogen phosphate(Merck, India)
- Hydrochloric acid (analytical grade)
- N-(3-Dimethylaminopropyl)-N′-ethylcarbodiimide hydrochloride (EDC) (Sigma Aldrich)
- 2-Aminoethyl methacrylate hydrochloride (Sigma Aldrich)
- *N*-Isopropylacrylamide (Sigma Aldrich)
- Potassium per sulfate (BDH)
- *N,N,N′,N′*-Tetramethyl ethylenediamine (Sigma Aldrich)
- Sodium Sulphide (Merck, India)

2.1.2 Instruments

Analysis of the samples was performed using the following instruments:

- Fourier Transform Infrared Spectrophotometer (SHIMADZU, FTIR-8400)
- Field Emission -Scanning Electron Microscopy (JSM-7600F, Tokyo, Japan)
- Centrifuge machine (Hettich, Universal 16A)
- pH meter (Hanna, HI 8424, Romania)
- Digital Balance (AB 265/S/SACT METTLER Toledo, Switzerland)
- Freeze dryer (Heto, FD3)
- Shaker machine (Stuart, Orbital shaker, SSL1)
- Oven (Lab tech, LDO-030E)

2.2 Methods of preparation

2.2.1 Synthesis of nano-starch particles (NSP)

Preparation techniques of NSP was optimized by varying acid concentration, MSP to acid ratio, hydrolysis time, temperature of hydrolysis and ultrasonic time and power. The hydrolysis was carried out at 5% to 18% (w/w) H_2SO_4 solution. NSP was formed at 18% (w/w) H_2SO_4 solution. A 500 mL round bottom flask containing 1 g of micro-starch particles (MSP) was placed in an oil bath at a 40°C temperature. Simultaneously, 100 mL 18 % (w/w) H_2S0_4 (NSP-to-acid weight ratio of 1 to 100) was adjusted to the desired temperature. When the two substances reached working temperature, H_2SO_4 was mixed with the starch, and the mixture was hydrolyzed at 40 ºC temperature for 210 minutes with continuous stirring with a magnetic stirrer [1]. The ultrasonication was applied during (every 15 minutes) the reaction while cooling in an ice bath to avoid overheating [2]. Immediately following hydrolysis, the suspension was diluted ten-fold to stop the reaction and allowed to settle for several hours to settle down the layer of the suspension. The clear top layer was through and then repeatedly washed with distilled water until they form separate layer. The suspension was then transferred into centrifuge tubes and repeated centrifugation was performed at 5,000 rpm for 15 minutes to remove excess acid and water-soluble fragments. The fine starch particles was dispersed in the aqueous solution approximately at pH 4. The opaque dispersion containing the polydisperse starch particles was then collected for further centrifugation at 5000 rpm for 45 minutes to separate the NSP suspension [3]. The suspension was then washed with distilled water. The process

was repeated four to five times for each sample to reduce the acid content. The purified NSP was kept in a refrigerator at 0°C for freeze dry and dried in freeze dryer for the preparation of powdered sample.

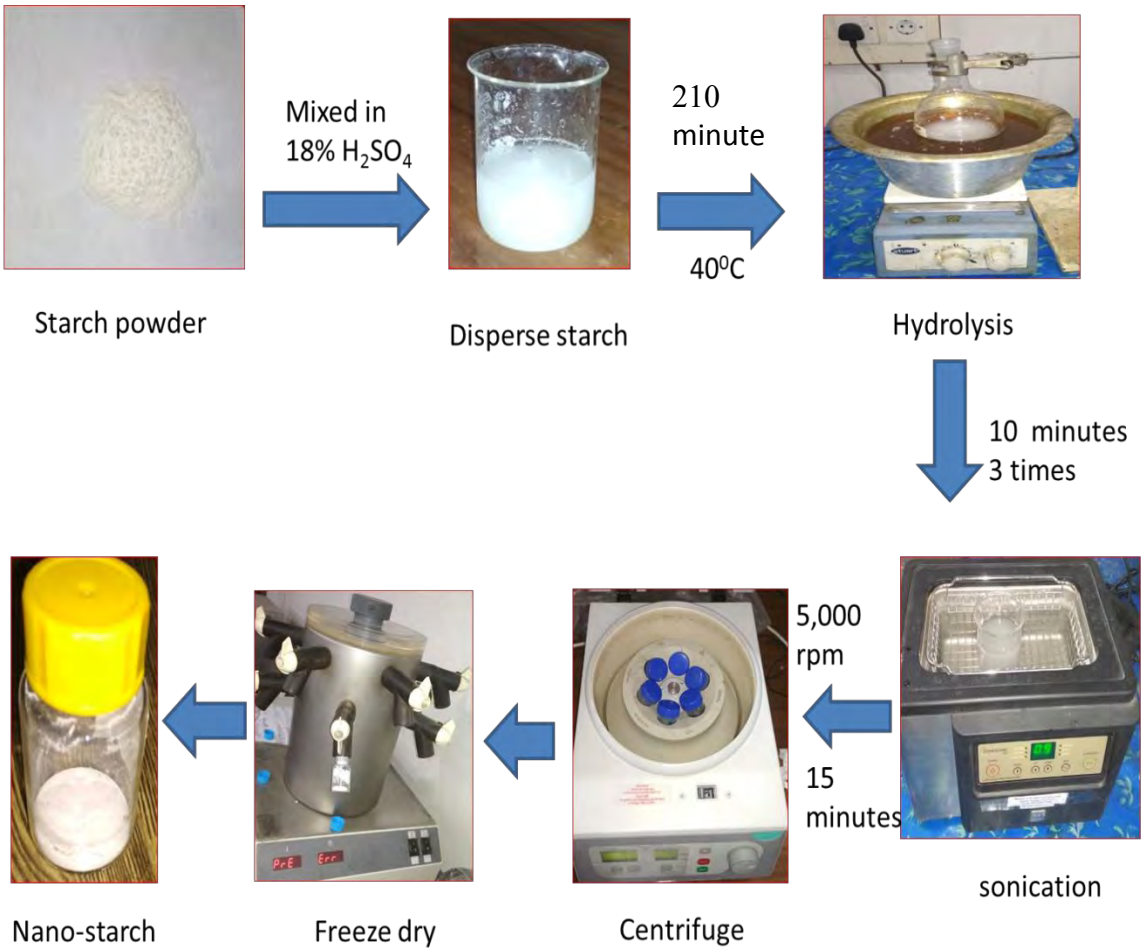

Figure 2.1 Schematic representations of synthesis of nano-starch particles from micro-starch.

2.2.2 Synthesis of carboxylated nano-starch (CNS)

The primary hydroxyl groups on the surface of NSP were oxidized to carboxyl groups using TEMPO-reagent in presence of sodium bromide and sodium hypochlorite. The reaction conditions were adjusted by following the previous studies [5-6]. 1g NSP was dispersed in 100mL distilled water. After vigorous mixing, sonication was performed for

10 min in an ice bath to get a homogeneous dispersion of NSP. 16 mg TEMPO and 100 mg NaBr were weighed and dissolved separately. After that mixed with NSP suspension and stirred 10 min at room temperature. The mixture was then further sonicated for 15 min. The oxidation was initiated with the addition of 3.5 mL of 4-14% NaClO solution to the NSP suspension by dropwise. The pH of the solution was maintained constant at 10 by adding 0.1M NaOH solution until no further variation was observed, indicating the completion of reaction. The solution was then continuously stirred for 12 h. Finally, 5mL of ethanol was added to stop the oxidation [4]. Then the solution was washed with distilled water several times and finally obtained concentrated suspension which was sonicated for 2 min and stored at 4^0C.

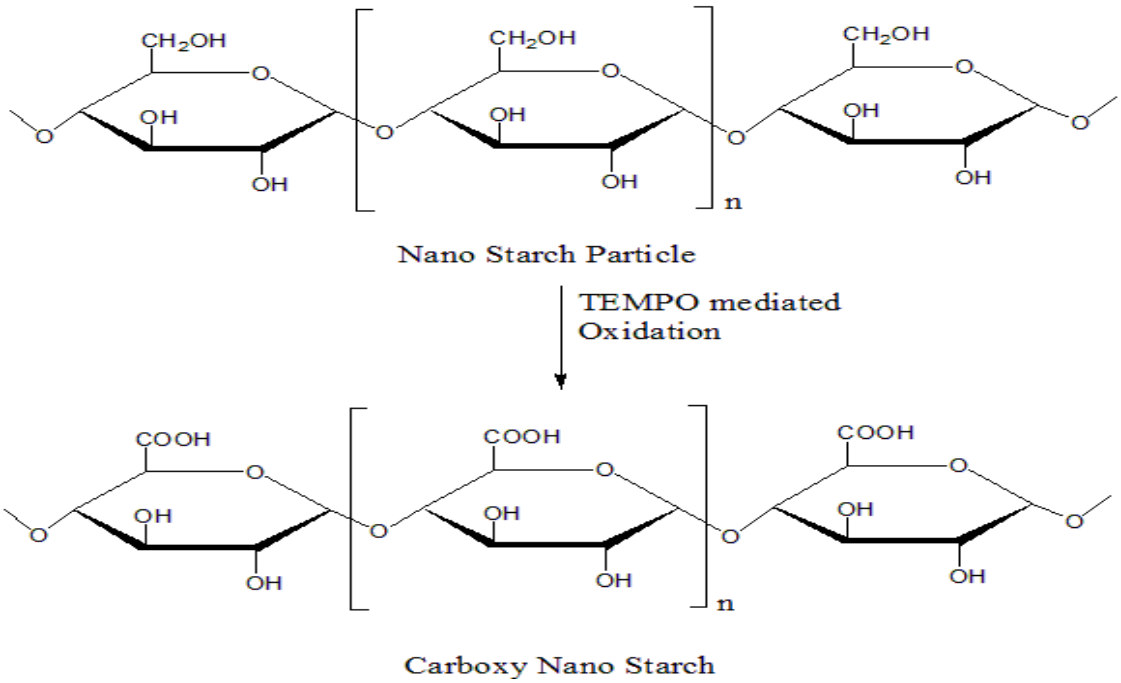

Figure 2.2 Schematic representation of synthesis of carboxylated nano-starch particles

2.2.3 Synthesis of modified nano-starch cross-linker (MNSC)

A 100 mL amount of 1.4 gL^{-1} CNS dispersion was mixed with 100 mL of PBS Buffer, and the pH of mixture was adjusted to pH=5 by adding 0.1 M HCl. To this mixture, 0.06 mmol of 2-aminoethyl methacrylate hydrochloride, 0.1 mmol of *N*-(3-dimethylaminopropyl)-*N′*-ethylcarbodiimide hydrochloride were added, and the pH was maintained at pH=5 while the mixture was stirred vigorously for 6 hours [7-8]. The mixture was dialyzed for 24h in

PBS buffer and then five days in distilled water. After dialysis, the amount of the modified nano-starch cross-linker was dried by using freeze drier and stored in a desiccator.

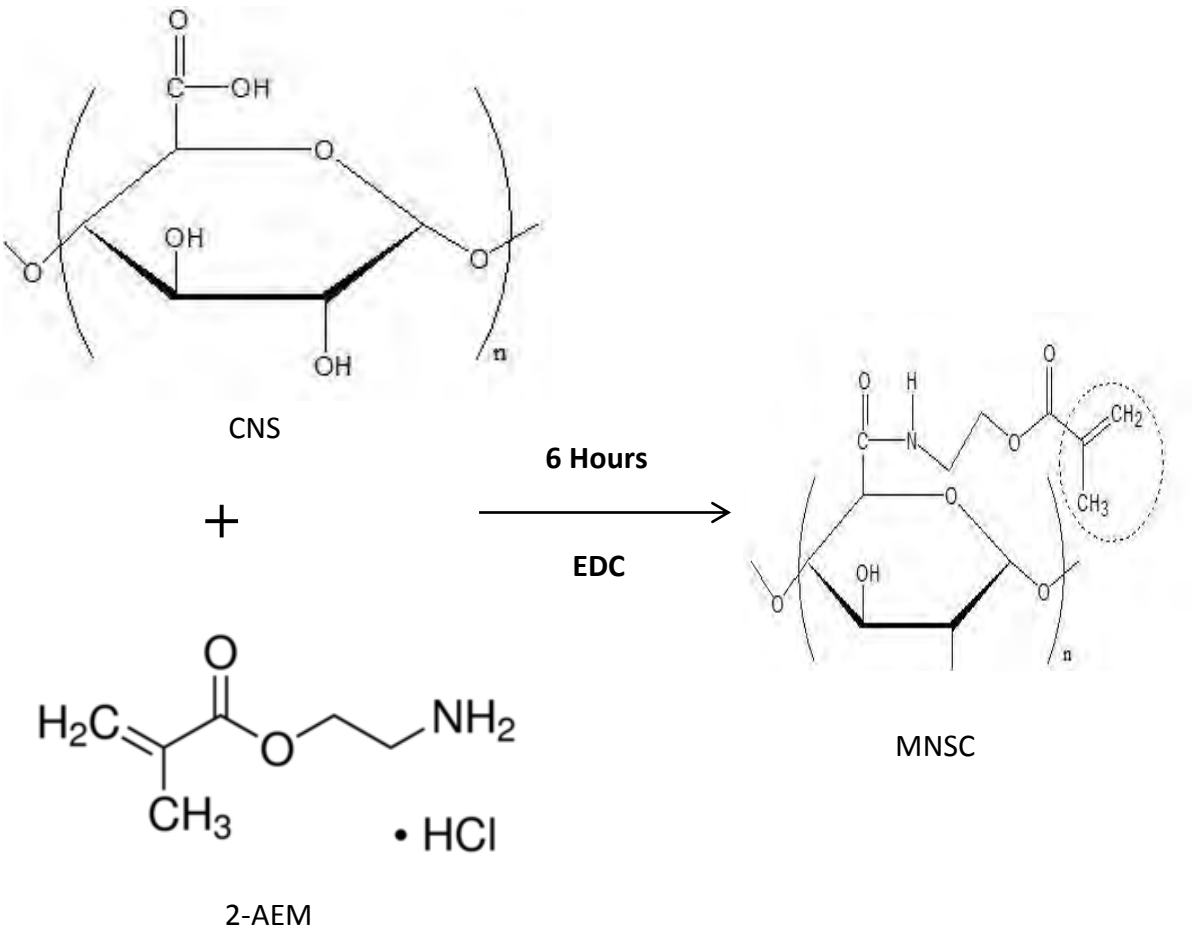

Fig. 2.3: Schematic illustration of preparation of MNSC

2.2.4 Synthesis of hydrogels using modified nano-starch cross-linker

The modified nano-starch cross-linker based hydrogel were prepared by the free radical polymerization of NIPAAM in presence of initiator KPS [9]. First, the modified nano-starch cross-linker was well dispersed in distilled water. Then was mixed with NIPAAM solution and sonicated for few minutes. Different amounts of MNSC were added to NIPAAM solution. Table 1 lists the different percentages of MNSC used in this work. Aqueous solution of varying amount of monomer and cross-linker was bubbled with N_2

gas to make the solution free from oxygen. A little amount of TEMED was mixed in solution which worked as accelerator for free radical polymerization reaction. In another container, the solution of initiator was bubbled with N_2 gas. Then two solutions were mixed immediately and transferred to a glass cell separated with a teflon spacer of desired shape and size. Glass test tubes also used for synthesis of cylindrical shapes hydrogel. Free radical polymerization of hydrogels was carried out at 2^0C for 24h in presence of KPS initiator. After polymerization, hydrogels were removed from teflon spacer or from glass tubes carefully. The hydrogels obtained in long cylindrical shapes were cut into pieces of approximately 13 mm length.

Table 2.1: Composition of different hydrogel precursors.

Crosslinker (MNSC)%	Monomer NIPAAM (g)	Initiator KPS (g)	Accelerator TEMED (µl)	Solvent H_2O (mL)
0.025	2	0.01	20	4
0.05	2	0.01	20	4
0.075	2	0.01	20	4
0.1	2	0.01	20	4

N-Isopropylacrylamide, modified nano-starch particle cross-linker and potassium persulphate were dissolved in water separately. A required amount of MNSC was taken in and mixed with NIPAAM, Then potassium persulphate was added in mixture at 2ºC. The polymerization reaction was occurred for 24 hours.

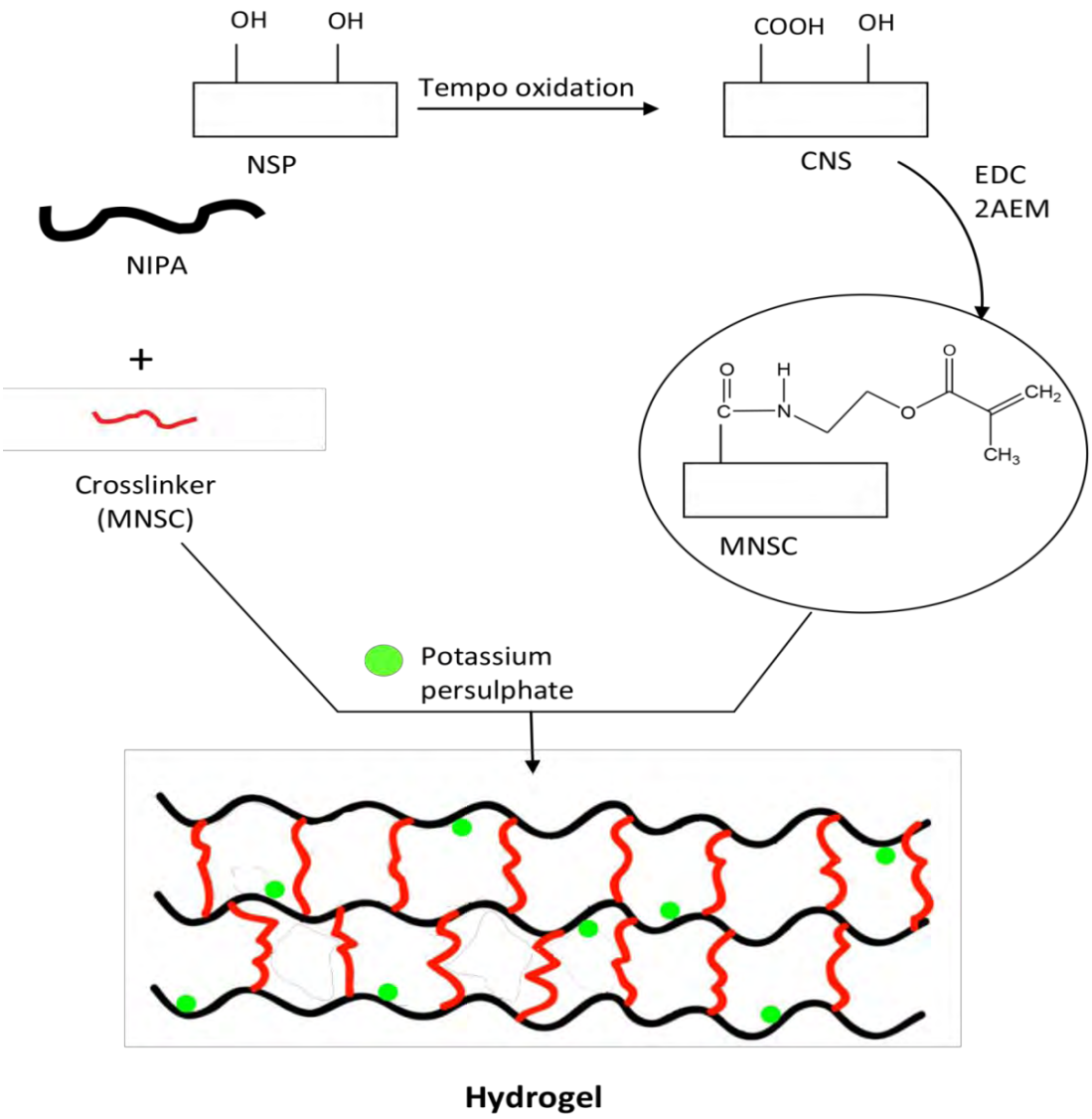

Fig. 2.4: Schematic representation of MNSC-NIPA hydrogel

2.3 Fourier Transform Infrared (FTIR) spectral analysis

The infrared spectra of the nano-starch particles, carboxylated nano-starch particles and modified nano-starch crosslinker samples were recorded by FTIR spectrometer in the region of 4000 – 400 cm^{-1}. 1 mg of NSP, CNS and MNSC were taken into vial and freeze dried. After that it was grinded as much as possible for FTIR analysis.

2.4.1 Field Emission Scanning Electron Microscopy (SEM)

The surface morphology of the MSP and synthesized NSP, MNSC were obtained using Field Emission Scanning Electron Microscopy (FE-SEM). The completely air dried samples were glued on a conducting carbon strip. The sample loaded strip was then mounted to a chamber that was evacuated to ~ 10^{-3} to 10^{-4} tor and then a very thin conductive platinum layer (few nanometers thick) were sputtered on the sample to ensure the conductivity of the sample surface. The sample was then placed in the sample chamber to view its surface. The microscope was operated at an accelerating voltage of 5.0 kV. The system was computer interfaced which provides recording of the surface images .

2.4.2 Energy Dispersive X-Ray Analysis (EDS)

An Energy Dispersive X-Ray Analyzer is used to provide elemental identification and quantitative compositional information. The atomic percentages of carbon, oxygen of nano-starch particle were confirmed by EDX analysis. Also the percentages of carbon, oxygen and nitrogen of modified nano-starch particle were confirmed by EDX analysis**.**

2.5 Nuclear magnetic resonance (NMR) spectroscopy

^{1}H NMR spectrum was recorded by Bruker BPX- 400 spectrometer operating at 400 MHz. DMSO was used as solvent and tetramethylsilane (TMS) as an internal standard. All chemical shifts (δ) were reported in ppm and coupling constants (*J*) in Hz. Chemical shifts were performed relative to tetramethylsilane (TMS) and *d*-solvent peaks (2.50 ppm in ^{1}H DMSO), respectively. Abbreviations used in the NMR experiments: s, singlet; d, doublet; t, triplet; q, quartet; m, multiplet.

2.6 Mechanical properties of hydrogel

Mechanical tests were conducted to assess the hydrogel properties. The mechanical properties of the hydrogels samples were measured by the Universal Testing Machine (UTM, Testresources, Model: 250-12 Actuator) at room temperature. Its load cell is 250 lb. For tensile and compressive tests, the hydrogels were cut into rectangular shape strips

(10-15 mm in length, 10 mm in width and 2 mm in thickness) and cylindrical (13 mm in diameter and 15 mm in height), respectively. The rate of stretching was set at 20 mm/min for tensile test and crosshead speed was fixed at 10 mm/min for compressive stress. It is noted that the compressive stress was measured at 70%. Different important mechanical property such as tensile strength, Young‟s modulus, ductility, toughness, elongation at break are calculated from the data of stress-strain curves and data of load-position curve. The experiments were repeated several times for reproducibility.

References

[1] Kumar, A., Negi, Y. S., Choudhary, V., Bhardwaj, N. K., "Characterization of cellulose nanocrystals produced by acidhydrolysis from sugarcane bagasse as agro-waste," *Journal of Materials Physics and Chemistry*, Vol. 2.1, pp. 1-8, 2014.

[2] Hee-Young, K., Dong, J. P., Jong-Yea, K., Seung-Taik, L., "Preparation of crystalline starch nanoparticles using cold acid hydrolysis and ultrasonication," *Carbohydrate Polymers,* Vol. 98, pp. 295–301, 2013.

[3] Bin, D., Peidong, S., Xinling, W., and Cheng, Y., "Preparation and properties of starch nanocrystals/ carboxymethyl chitosan nanocomposite films," *Starch/Sta¨rke,* Vol. 63, pp. 528–535, 2011.

[4] Jun, Y., Chun-Rui, H., Xue-Ming, Z., Feng, X., and Run-Cang, S., "Cellulose Nanocrystals Mechanical Reinforcement in Composite Hydrogels with Multiple Cross-Links: Correlations between Dissipation Properties and Deformation Mechanisms," *Macromolecules,* Vol. 47.12, pp. 4077-4086, 2014.

[5] Wolfgang, A. H., Alexandra, M. J. R., Evangeline, T., Herbert, R., and Fritz, E. K., "Super absorbers from renewable feedstock by catalytic oxidation," *Green Chem.,* Vol. 10, pp. 442–446, 2008.

[6] Yan-fang, H., Xiao-dong, Z., Zhao-guang, N., Ya-cheng, X., Bo-qun, L., and Li-li S., "Selective Oxidation of Corn Starch in TEMPO-Mediated System," *Advanced Materials Research,* Vol. 1051, pp. 221-224, 2014.

[7] Erdem, K., Torbjo, P., Mikael, A., and Lars, W., "Adhesive Layer-by-Layer Films of Carboxymethylated Cellulose Nanofibril Dopamine Covalent Bioconjugates Inspired by Marine Mussel Threads," *karbulutetal.*, Vol. 6, pp. 4731–4739, 2012.

[8] Perreux, L., Loupya, A.,' and Volatronb, F., "Solvent-free preparation of amides from acids and primary amines under microwave irradiation," *Tetrahedron,* Vol. 58, pp. 2155-2162, 2002.

[9] Frances, Y. P., Lee, M., Jessica, R. B., and Nolan, T. F., "Thermoresponsive Behavior of Poly(N-Isopropylacrylamide) Hydrogels Containing Gold Nanostructures," *Langmuir,* Vol. 22, pp. 3851-3857, 2006.

CHPTER 3
Results and Discussion

3.1 Synthesis of nano-starch particle

Starch is the most common carbohydrate in the human diet and is contained in many staple foods. Nano-starch particle was synthesized from starch granule. Sizes of starch granules are micro level. Micro starch particle are cheap, easily available and a new source of NSP. So, for environmental safety and also for industrial purposes, NSP obtained from starch granule creates a new dimension. NSP is usually synthesized by acid hydrolysis process [1]. A complete set of experiments were performed to examine the formation of transparent NSP after acid hydrolysis. Here, 5% to 18% H_2SO_4 solution were used for hydrolysis purpose. The acid concentration less than 18% gave white powder similar to starting MSP. On the other hand acid concentration more than 18% gave blackish product; it may be due the carbonization of starch. These finding gave us an indication to choose 18% sulfuric acid concentration for hydrolysis purpose and at this concentration the product formed well dispersion in medium.

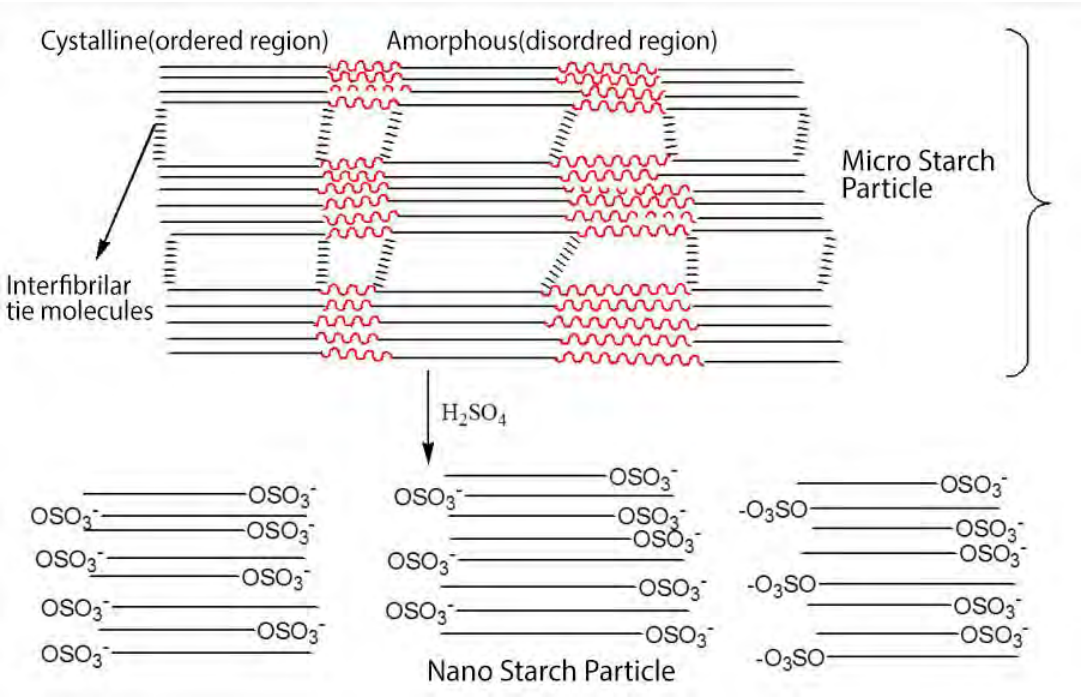

Figure 3.1 Schematic representation of nano-starch particles formation

Similarly, acid to MSP ratio, temperature of the hydrolysis and time for hydrolysis were also investigated and the results from those studies gave indication to choose the optimum condition for hydrolysis. The optimum condition of hydrolysis was carried out at 40°C temperature for 210 minutes with 18% (w/w) H_2SO_4 at the acid to NSP ratio 100: 1 [2]. NSP was well dispersed which was treated by ultrasonic treatment. The ultra-sonication effectively fragmented starch hydrolyzes to nanoparticle. Starch particle contains both amorphous and crystalline region. The pH of the solution was maintained almost neutral by several times centrifugation of acid hydrolysis solution. After hydrolysis the diameter and size of hydrolyzed starch was reduced to great extent due to removal of most the amorphous region of microcrystalline starch and finally nano-starch particle was obtained. A wide range of hydroxyl groups on the surface of NSP are responsible for tightly bonded hydrogen networks [3]. Nano starch particle has several notable chemical optical and electrical properties. Their size, shape lead to unique behavior in solutions [4-5] and its surface is highly chemical reactive. The starch nanoparticles could be prepared with high yield (70%).

3.2 Surface morphology study of nano-starch particle using Scanning electron microscope

Scanning electron microscopy is an effective way to observe the morphology of particles. The surface morphology of synthesized micro starch particle and NSP were studied by FE-SEM. After hydrolysis the diameter and size of hydrolyzed starch was reduced to great extent due to removal of most the amorphous region of microcrystalline starch leaving nano-scale spherical crystals. From Fig. 3.2(a), the FESEM image of starting MSP, it can be mentioned that MSP particles were irregular spherical shapes and their average size was about 10 μm. The irregularity may be due to the presence of more amorphous region in MSP compare to NSP. Fig. 3.2(c) shows the FESEM micrographs of nano-starch granule, which revealed that the starch nano particles have spherical shapes with diameters ranging from 80 to 200 nm. The ultrasonic treatment increased the transparency of starch suspension as a result from the size reduction of suspended particles. The dispersion of starch showed a decrease in viscosity but increase in solubility and clarity. SEM verified that the acid hydrolysis and ultrasonic treatment produced well defined nanoparticle [6]. Fig. 3.2(c) shows that the morphology of starch nanoparticles was highly uniform and not affected by the hydrolysis conditions tested [7]. Their compact agglomeration of NSP

shows that starch chains have an intermolecular hydrogen bonding and a strong hydrophilic interaction in between the starch chains. Micro starch has thus successfully converted into nano-starch particle.

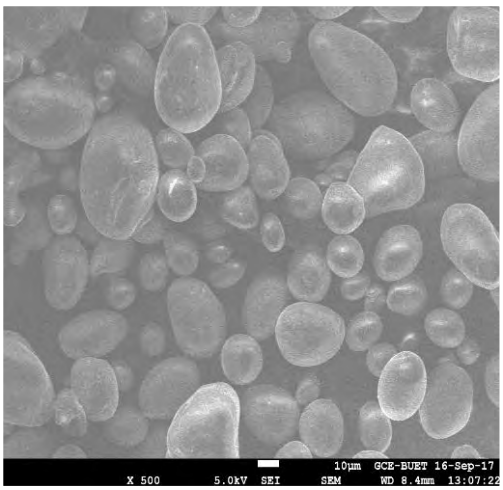

a

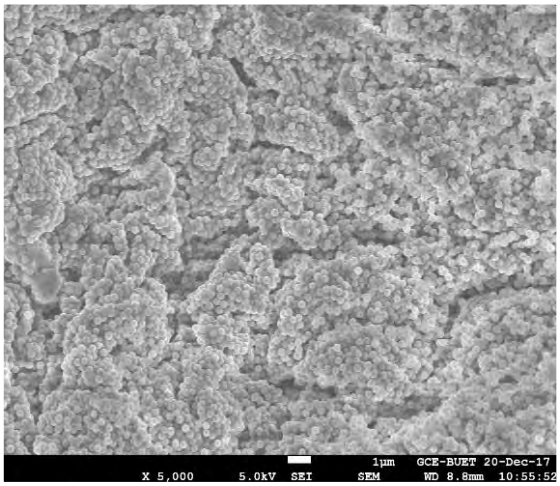

b

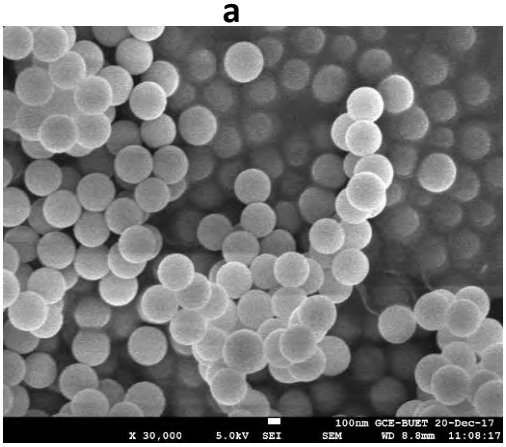

c

Figure 3.2: SEM image of (a) MSP with magnification x 500 (b) NSP with magnification x 5000 and (c) NSP with magnification x 30000

3.3 Energy-Dispersive X-ray Spectroscopy Analysis of Nano-starch Particle

Carbon and oxygen were found in NSP which were confirmed (Fig. 3.3) by EDS elemental analysis. NSP structure consists of only carbon and oxygen. The EDS elemental analysis, which is given in Table 3.1, reveals 71.13%, 28.87% (mass) and 76.65%, 23.35% (atom) for C, O, respectively. This analysis confirms the presence of carbon and oxygen containing functional groups on the surface of NSP.

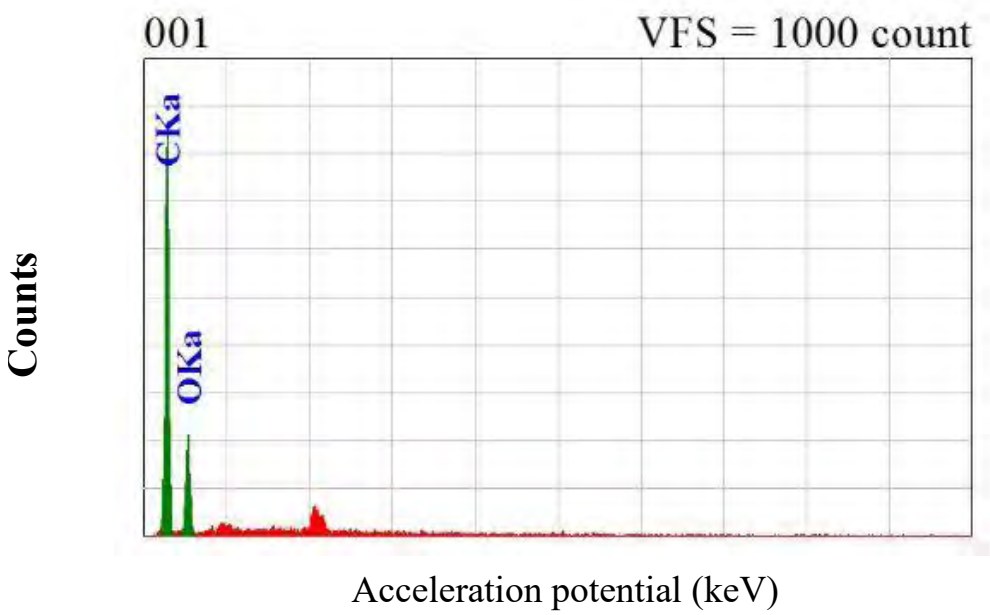

Figure 3.3: EDS spectra of NSP

Table. 3.1: EDS elemental analysis of NSP

Element	Acceleration potential (keV)	Mass%	Atom%
C	0.277	71.13	76.65
O	0.525	28.87	23.35

3.4 Carboxylate nano-starch particle preparation

Carboxylate nano-starch particle was prepared by a TEMPO mediated oxidation. A wide range of hydroxyl groups of NSP are tightly bonded by hydrogen bond. These hydrogen bonds can be loosen through increasing the electrostatic repulsion and adsorption ability. Primary hydroxyl groups of NSP are converted to carboxyl groups and this carboxyl groups containing NSP is denoted here as carboxylate nano-starch. This conversion is carried out by 2, 2, 6, 6-tetramethylpyperidine-1-oxyl mediated oxidation [8]. In this process, TEMPO is used as primary oxidant and sodium hypochlorite as secondary oxidant. Figure 3.4 Shows mechanism of TEMPO mediated oxidation process. During this process NaBr is used to increase the rate of oxidation through the formation of sodium hypochlorite. At pH < 8, the reaction proceeds slowly and selectivity between primary and secondary alcohols which is not as prominent as at 9 < pH < 11. At 9 < pH < 11, the reaction shows good selectivity to primary alcohol [9-10]. After TEMPO mediated oxidation process carboxylate groups are successfully formed.

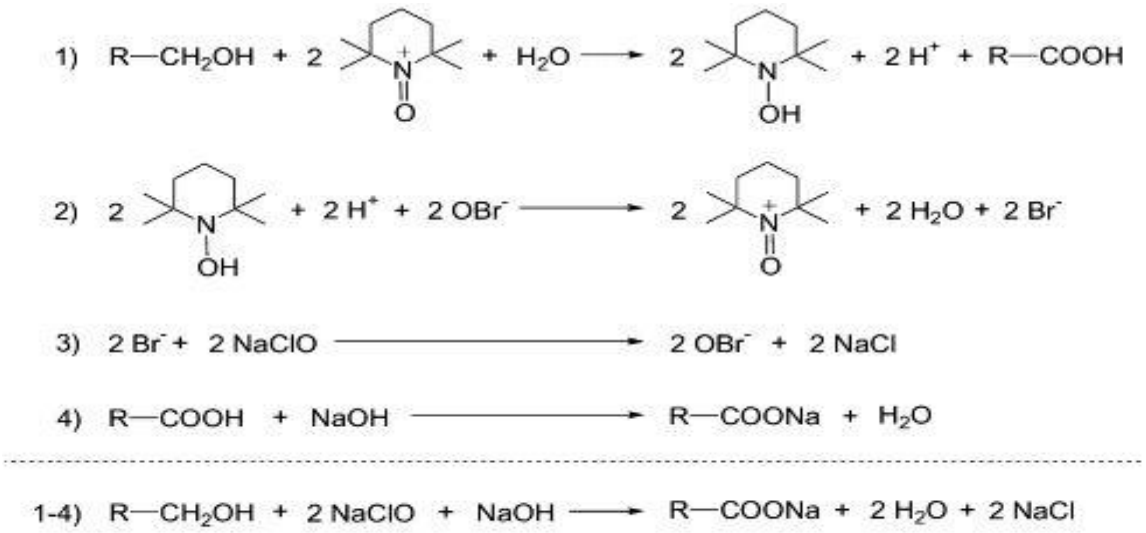

Figure 3.4: Formulae for oxidation of primary hydroxyl groups of nano-starch particles to carboxylated nano-starch particles via TEMPO mediated oxidation.

3.5 Synthesis of modified nano-starch cross-linker

Physiochemical properties of CNS are different from nano-starch particles. The resulting chemically modified of nano-starch could then potentially become much more suitable for many applications. There are many ways by which CNS can be functionalized. Carboxylates (-COOH) reacts with primary amines (-NH_2) of 2-aminoethyl methacrylate hydrochloride in presence of 1-ethyl-3-(3-dimethylaminopropyl)-carbodiimide (EDC) and forms carbamide bond between CNS and 2-aminoethyl methacrylate hydrochloride. In presence of EDC as a coupling agent, the coupling reaction occurrs to obtain vinyl modified nano-starch cross-linker in solution. The amino (-NH_2) group of 2-aminoethyl methacrylate hydrochloride and the carboxyl(-COOH) group of CNS are reacted and formed carbamide (CONH) group [11-12]. Fig. 3.5 shows that modified nano-starch cross-linker contains active vinyl group which is able to work as a cross-linker to synthesize hydrogel.

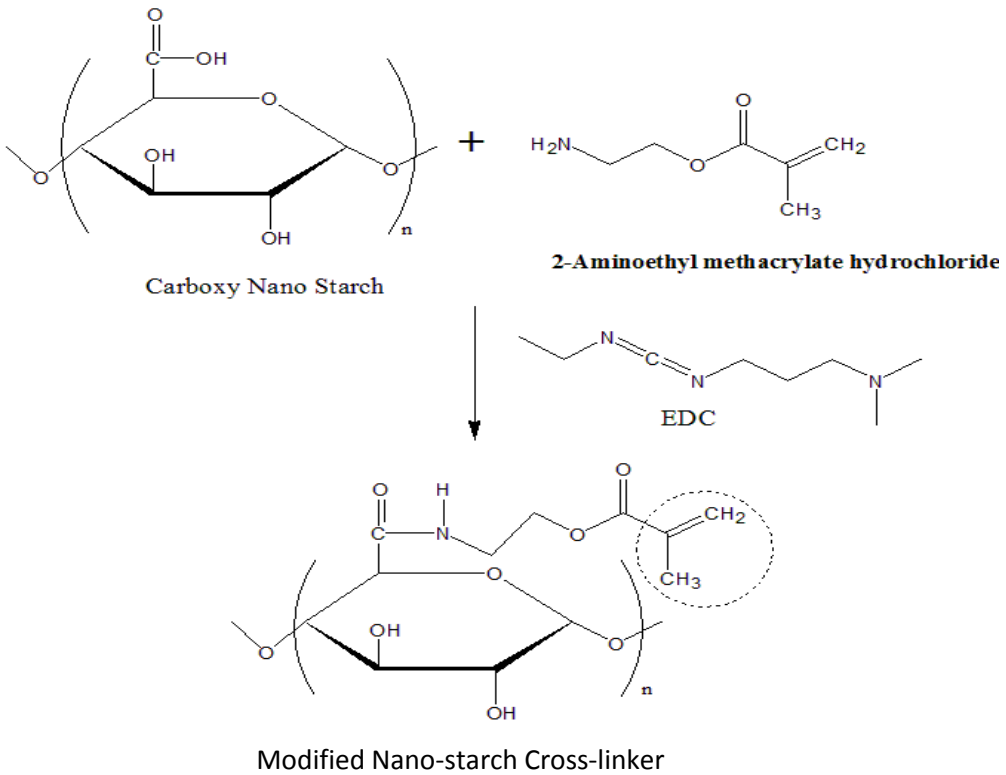

Fig. 3.5: Schematic representation of the structure of a modified nano-starch cross-linker (MNSC)

3.5.1 Study of surface morphology of MNSC using Field Emission Scanning Electron Microscopy

Surface morphology of prepared MNSC is further studied from the SEM analysis. The SEM images of MNSC are shown in Fig. 3.6: (a) & (b) respectively. MNSC nanoparticle is more uniform, homogeneous due to proper modification of carboxylated nano-starch particles. Maximum particles are irregular in shape with a size ranging from 80 to 200 nm.[13-15].

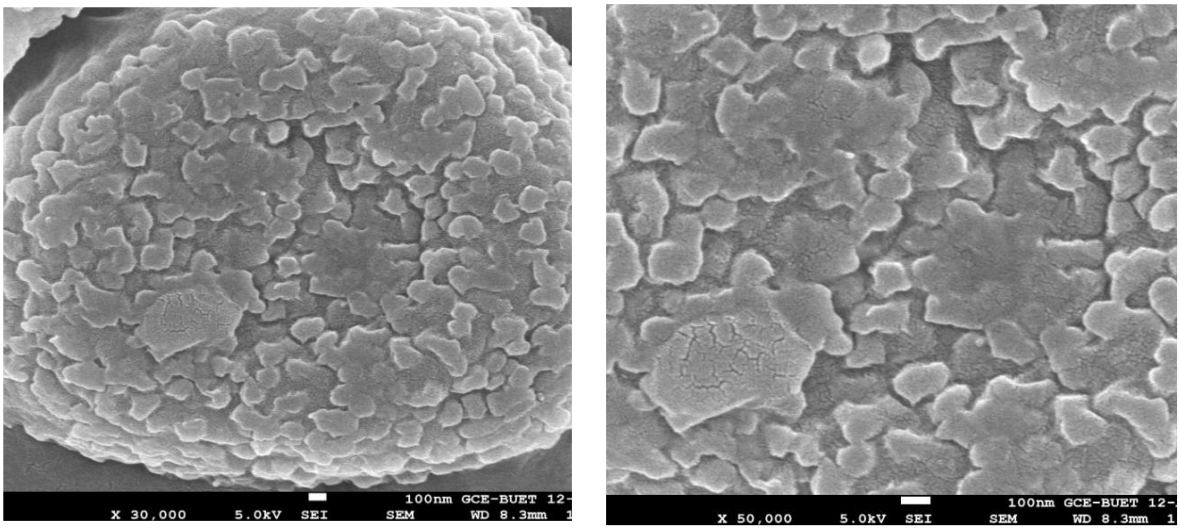

a b

Fig. 3.6: SEM image of a) MNSC with magnification×30,000 and b) MNSC with magnification×50,000

3.5.2: Energy-Dispersive X-ray Spectroscopy analysis of MNSC

The EDS elemental analysis confirmed (Fig. 3.7) the presence of carbon, oxygen and nitrogen in MNSC. Table 3.2 reveals that the amount of C, N and O in MNSC are 77.19%, 8.45%, and 14.36% (mass) and 81.07%, 7.61%, and 11.33% (atom), respectively. This analysis confirms the presence of nitrogen in MNSC which is introduced comes after coupling reaction.

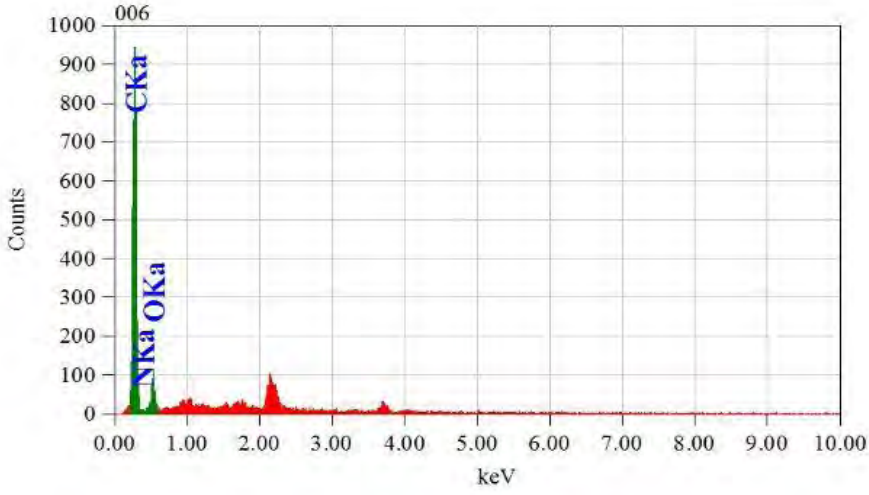

Fig. 3.7: EDS spectra of MNSC

Table 3.2: EDS elemental analysis of MNSC

Element	Acceleration potential (keV)	Mass%	Atom%
C	0.277	77.19	81.07
N	0.392	8.45	7.61
O	0.525	14.36	11.33

3.6 Functional group investigation by Fourier Transform Infrared Spectroscopy

In the FT-IR spectra of the nano-starch, NSP and MNSC are shown in Fig.3.8. The wide absorption peaks band near 3411 cm^{-1} comes from the stretching vibration of the - OH in the starch. Absorption band at 2930 cm^{-1} belongs to the stretching vibration of saturated C - H in the starch. The band at 1643 cm^{-1} belongs to the shear vibration of the two - OH of the water absorbed by the starch. The absorption band at 1383 cm^{-1} is due to the bending vibration of the methyl C – H. The peaks at 1157, 1080 and 995 cm^{-1} are the stretching vibration absorption bands of the C - O - C of the starch. The remarkable band in the figure at 1730cm^{-1} confirms the presence of C=O bond [16].

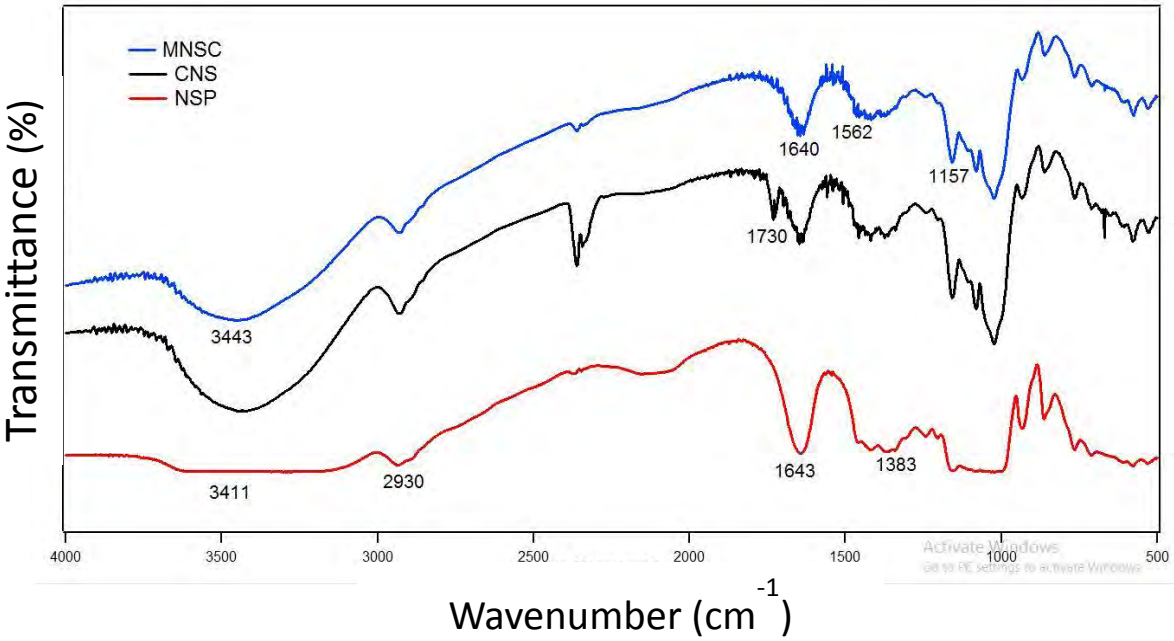

Fig. 3.8: FTIR spectra of nano-starch particle, carboxylated nano-starch, modified nano-starch cross-linker

In case of MNSC, a band at 3443cm^{-1} attributes to N–H stretching which overlapped with a broad band from carboxylic acid stretching, can be seen. Two bands at 1562 and 1157 cm^{-1} attributes to N–H bending and C–N stretching vibrations.

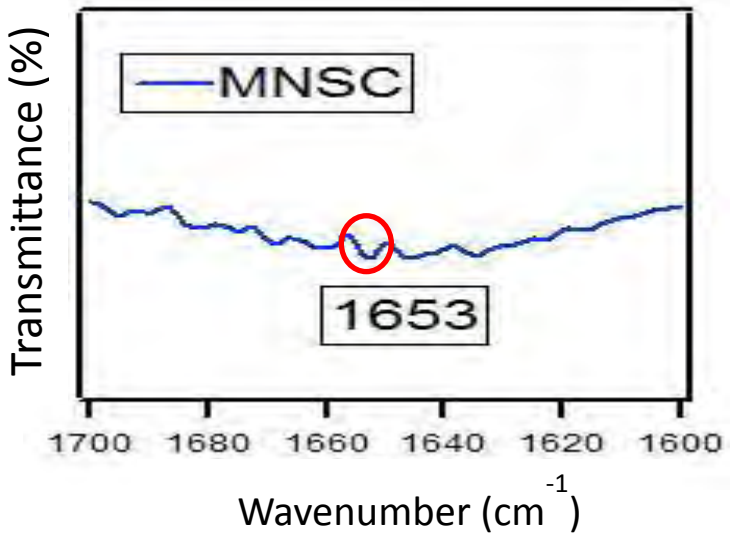

Fig. 3.9: FTIR spectra of modified nano-starch cross-linker after magnification in the region of 1600-1700 cm^{-1}

Figure 3.9 shows that the 1635cm^{-1}-1660cm^{-1} two bands are overlapped with each other. One is 1640 cm^{-1} which is originated from C=O for amide and 1653cm^{-1} which is for C=C stretching vibrations. The peak at 1640 cm^{-1} corresponds to stretching vibrations of NHCO bond. Hence, FTIR analysis confirms the successful modification of CNS by 2-aminoethyl methacrylate hydrochloride to obtain MNSC [13-17].

Table 3.3: Characteristic peaks of NSP, CNS and MNSC in FT-IR spectra

Wavenumber (cm^{-1})	Vibration type	Wavenumber (cm^{-1})	Vibration type
3411	OH stretching	3443	NH stretching
2930	CH stretching	1640	stretching
1643	OH for water absorption	1562	NH plane stretching
1383	CH bending	1157	CN stretching
1730	C=O of carboxylic	1653	C=C stretching

3.7 Nuclear magnetic resonance analysis

The ^{1}H-NMR spectrums (Fig. 3.10) of MNSC exhibits peaks (in δ ppm) as follows:

- ✓ 5.53-5.39 (2H, vinyl) : two vinyl protons at (C-3)
- ✓ 5.10-5.01 (m, 1H) : one proton at (C-16)
- ✓ 4.57-4.51 (m, 2H) : two protons at (C-6)
- ✓ 3.65-3.58 (m, 5H) : five protons at (C-5, 9, 10, 16)
- ✓ 3.47-3.36 (m, 2H) : two protons at (C-12, 15)

The total forty (40) proton atoms were obtained in the compound by ^{1}H-NMR spectrum. The ^{1}H-NMR data confirms the structure of MNSC as shown below:

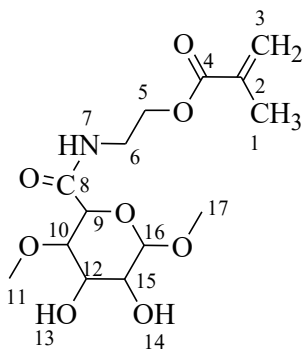

Figure 3.10: Structure of MNSC cross-linker (One glucose unit is depicted for clarity)

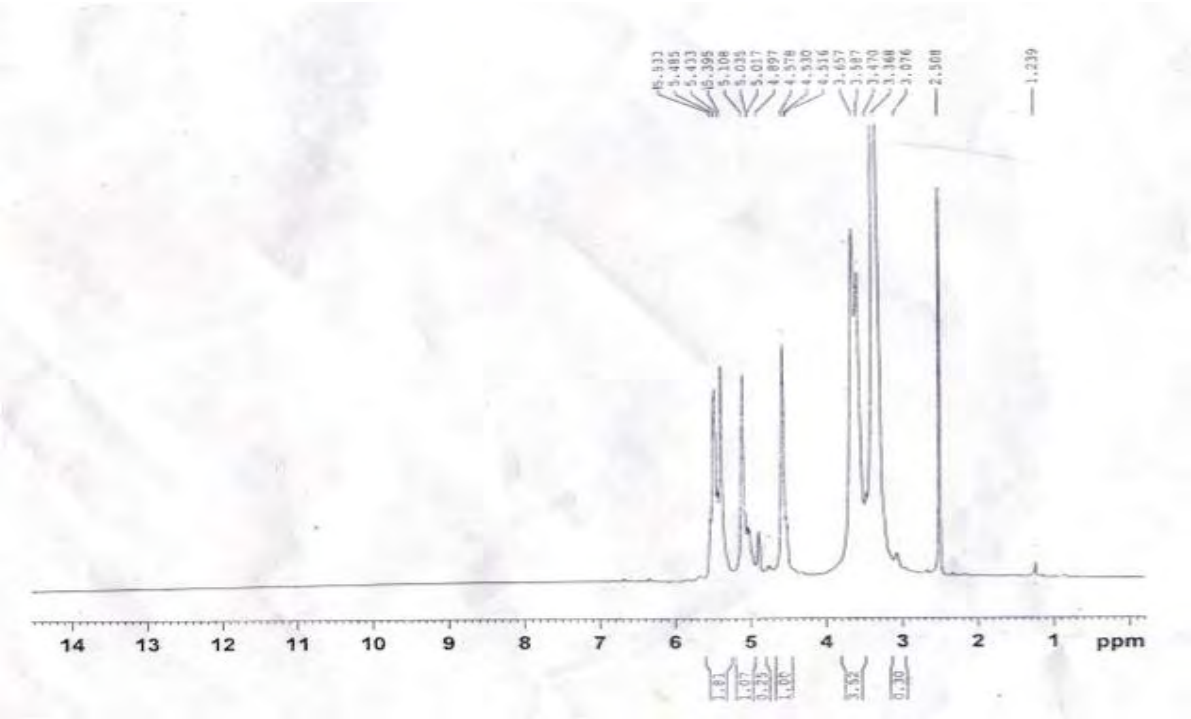

Figure 3.11: ^{1}H-NMR spectrum of synthesized MNSC cross-linker

Figure 3.11 testifies the presence of vinyl group in MNSC compound whose chemical shift is δ= 5.53-5.39.

3.8 Synthesis of modified nano-starch cross-linker based cross-linked Poly (*N*-isopropylacrylamide) (MNSC-NIPA) hydrogel

The key point of this approach relies on good dispersion of cross-linker in solvent, followed by in situ polymerization initiated at 2^{0}C. As the MNSC cross-linker can be thoroughly dispersed in water, it is suitable to be used for preparation of hydrogel. MNSC based cross-linked polymer hydrogel is prepared through in situ polymerization technique of NIPAAM monomer with MNSC cross-linker in presence of KPS initiator [18-20].

3.8.1 General reaction mechanism of free radicle polymerization for MNSC-NIPA hydrogel

Figure 3.12 represents reaction mechanism of free-radical polymerization. Here KPS is expressed as R. When energy is supplied to KPS, it decomposes homolytically and spilts into two symmetrical compounds and two fragments, each carrying one unpaired (lone) electron that is called free-radical. Initially, the highly reactive free-radical attacks the double bond of a NIPAAM monomer. π electrons of C=C molecules are not too close to the nucleus. For this reason π electrons are easily attacked by free radical electron and form sigma bond between initiator and monomer species by one electron from initiator and other is from π bond electron of C=C molecules. Another π electrons of π bond of C=C molecules is easily transferred to the other end of monomer. Again radical site of the first monomer unit attacks the double bond of another fresh monomer molecule. They are linking up second to first monomer unit. This process continues and attacks on fresh monomer molecules to propagate polymer chain length.

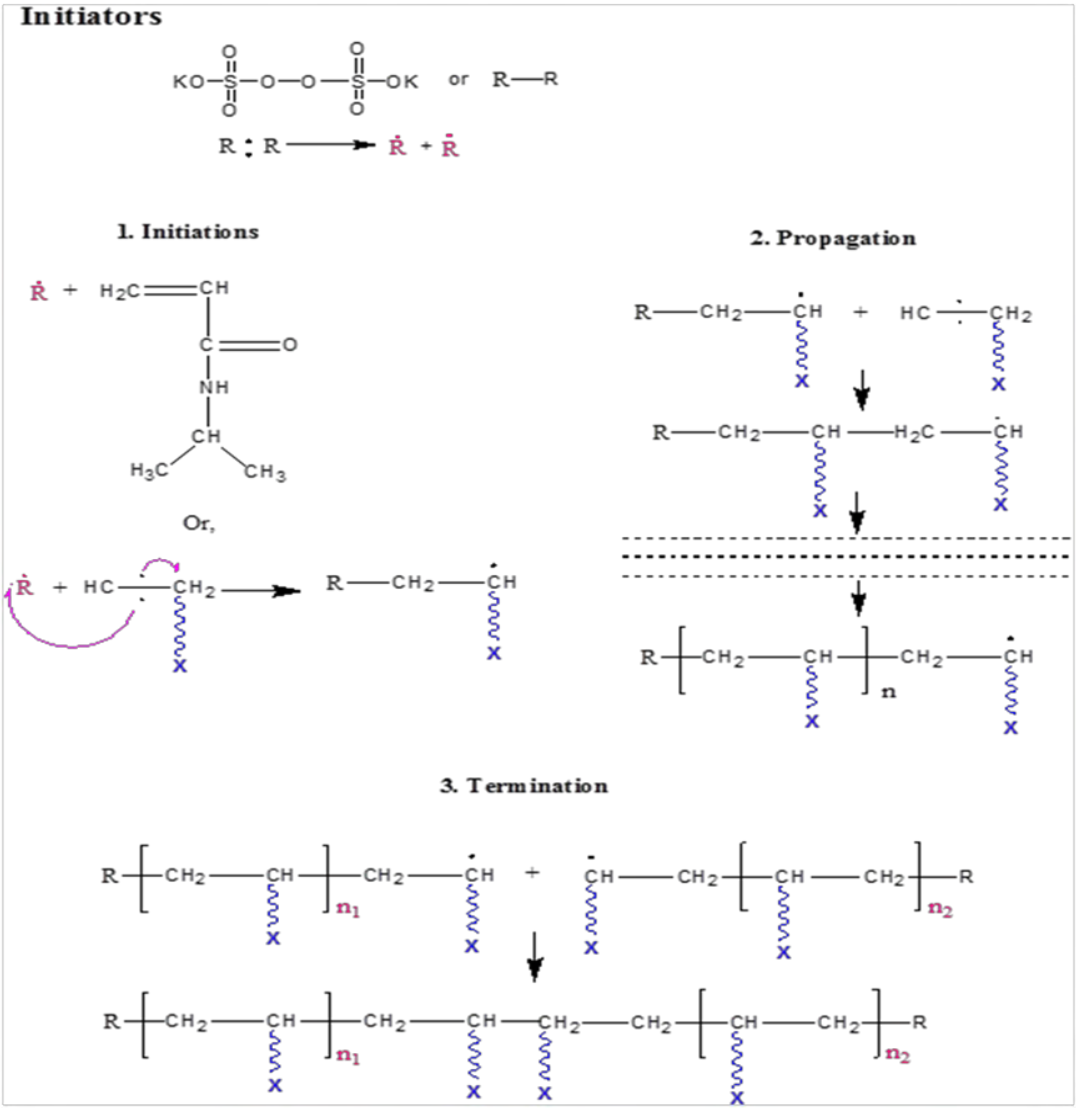

Figure 3.12: Reaction mechanism of free radical polymerization of MNSC-NIPA hydrogel

At the termination, the monomer unit to the growing chain is stopped and growth of the polymer chains arrested. Finally two growing chain units are added by the coupling of the presence of lone pair electron. Thus their reactiveness is nullified. This termination is known as termination by coupling.

Figure 3.13 also represents the proposed structure of MNSC-NIPA hydrogel. The crosslinking of MNSC is well established with NIPAAM polymer chain at 2^0C. MNSC contains vinyl group which is able to form covalent bond with NIPAAM polymer chain by

free-radical polymerization. MNSC cross-linkers are chemically joined among polymer chains and formed polymer network.

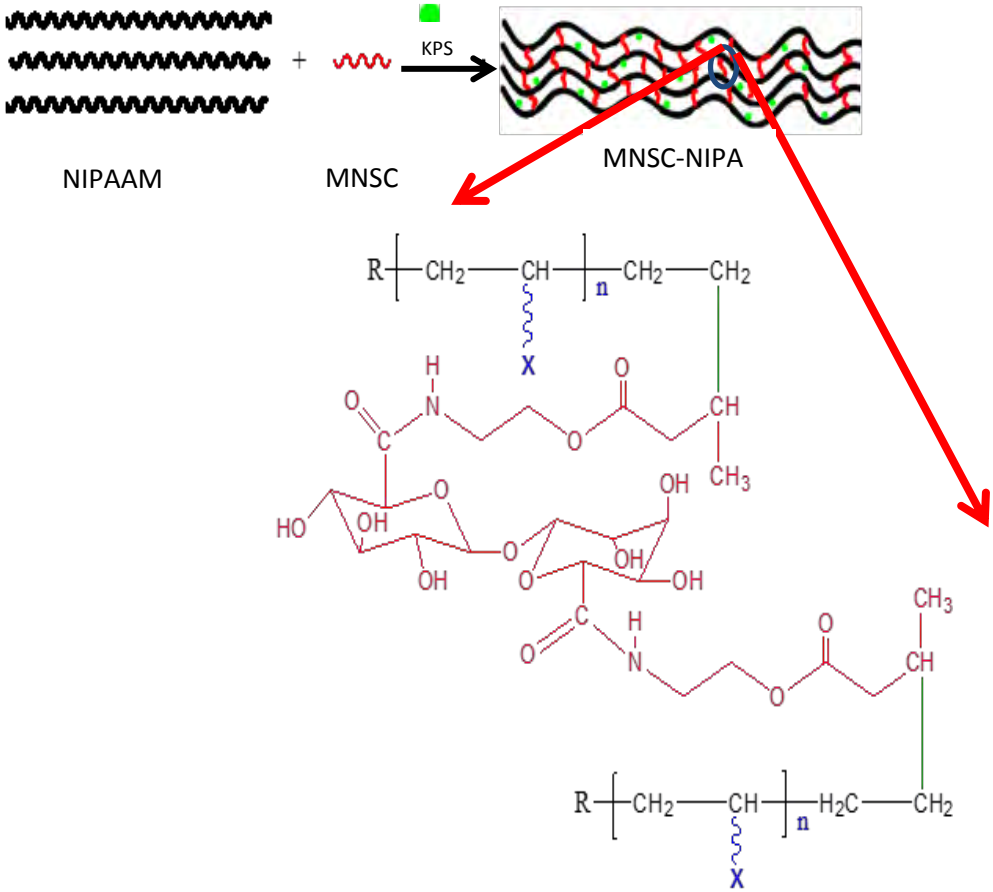

Fig. 3.13: Chemical structure of MNSC-NIPA hydrogel (For the sake of clarity only one glucose unit is depicted)

3.9 Mechanical Properties of MNSC-NIPA hydrogels:

Most mechanical analysis of hydrogels are conducted from stress-strain curve during elongation and compression. At present the most commonly used method to determine the mechanical properties of hydrogels are by elongation and compression. Both methods have been extensively used to study the mechanical behaviors of various hydrogels [21-22]. For both tension and compression, the original load vs displacement curve is converted to stress-strain data using simple geometrical relationship.

3.9.1 Mechanical Properties of MNSC-NIPA hydrogels for elongation

Elongation of hydrogel is important for evaluation of different mechanical properties. It measures how much elongated from initial length without breaking. Elongation testing is used to find many important properties. Rectangular shape MNSC-NIPA hydrogels are prepared with 2 mm thickness for elongation test [23]. The photo in Figure 3.14 represents the elongation process of hydrogel. The initial length of hydrogel is 14 mm and finally gets 226 mm after elongation which is 16 times elongated from its initial length. Different mechanical properties are calculated from stress-strain curve.

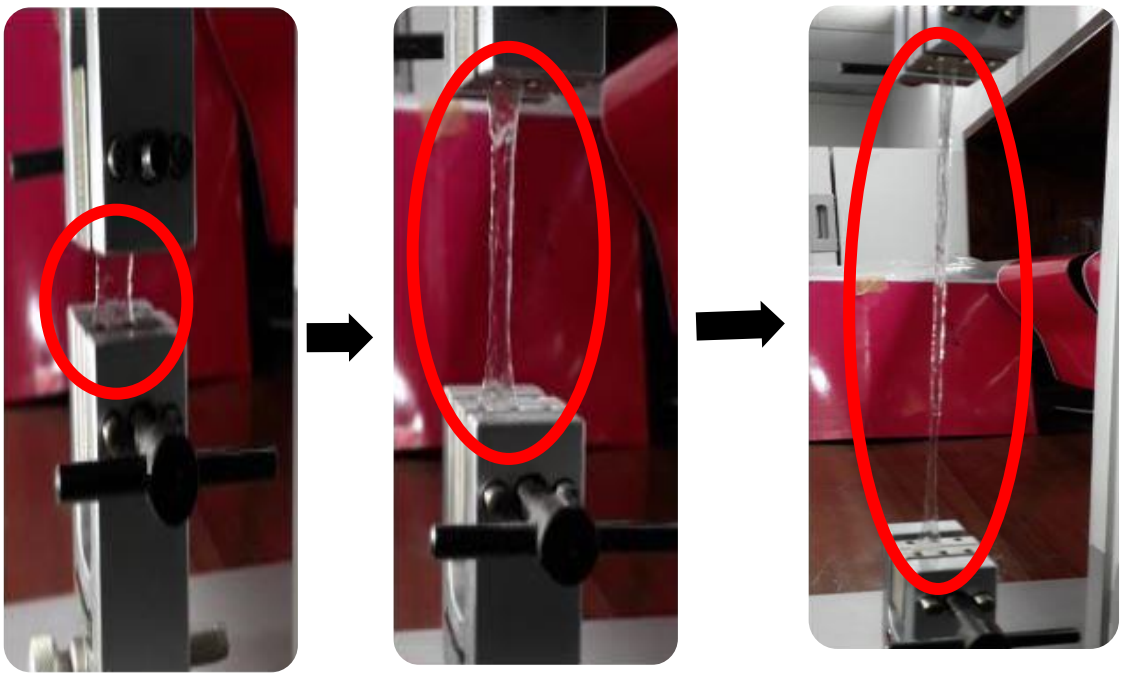

Fig. 3.14: Elongation process of MNSC-NIPA hydrogel. The elongation at break for MNSC-NIPA hydrogel is very high.

The real stress-strain curves for as prepared MNSC-NIPA hydrogels obtained from the data generated from the load-position curve obtain by the instrument. Fig. 3.15 shows individual mechanical properties of MNSC-NIPA hydrogels using different amount of cross-linker. Four samples of MNSC-NIPA hydrogels are characterized by typical non-linear stress-strain variations before their rupture.

.

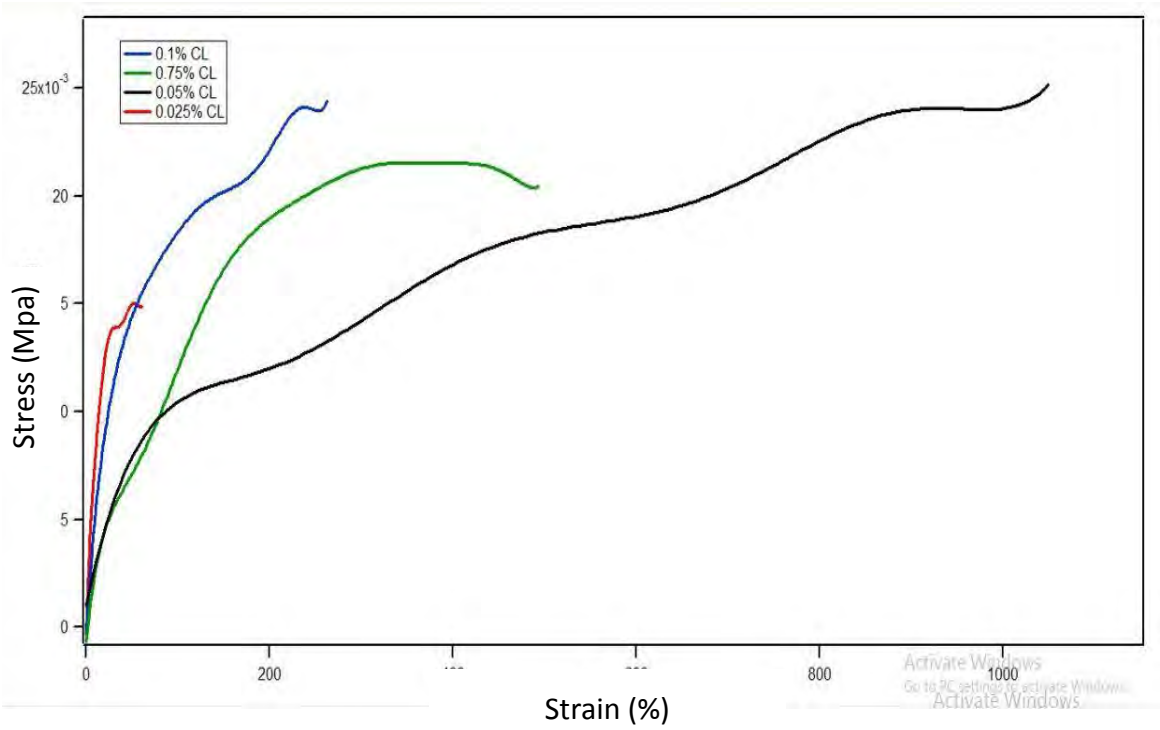

Fig. 3.15: Stress-strain curves of MNSC-NIPA hydrogel for Elongation

Ultimate tensile strength could directly be recorded from the highest point of stress-strain curve during experiment. Fig 3.16 shows that the tensile strength is gradually increased due to increasing amount of cross-linker. At the amount of 0.05% cross-linker is well dispersed in solvent. As a result, MNSC distributed among all of the polymer chain and cross-linker take place homogenously in the polymer matrix. Tensile strengths are approximately same for amount of 0.1% and 0.05% MNSC.

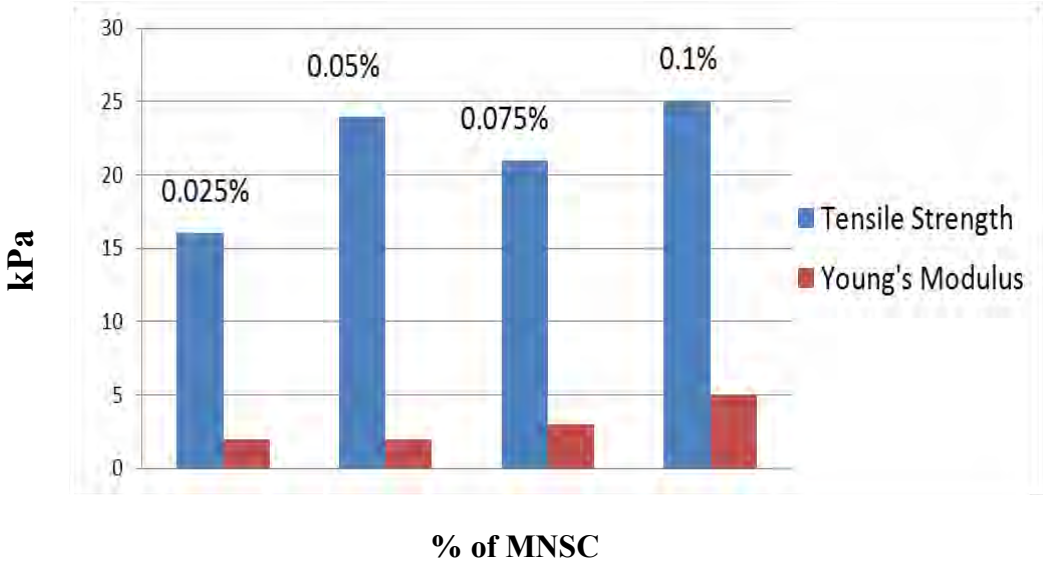

Fig. 3.16: Tensile strength and Young‟s Modulus of MNSC-NIPA hydrogel for elongation

Table 3.4: Tensile strength and Young‟s modulus of MNSC-NIPA hydrogel

Amount of cross-linker (%)	Tensile strength (kPa)	Young's Modulus(kPa)
0.025	16	2
0.05	24	2
0.075	21	3
0.1	25	5

Fig 3.16 shows that Young‟s modulus is low when 0.05% and 0.025% MNSC cross-linker are used. Young‟s moduli increase due to increasing the amount of cross-linker. Fig 3.14 also suggests that elongation at break for MNSC-NIPA hydrogel increases due to increase of cross-linker amount. When 0.025% cross-linker is used, MNSC-NIPA readily breaks at lower concentration. It has lower deformation in elongation and elongation at break at

446%. On the other hand when cross-linker amount was 0.05% it shows totally different enhanced tensile behavior than lower 0.025% cross-linker.

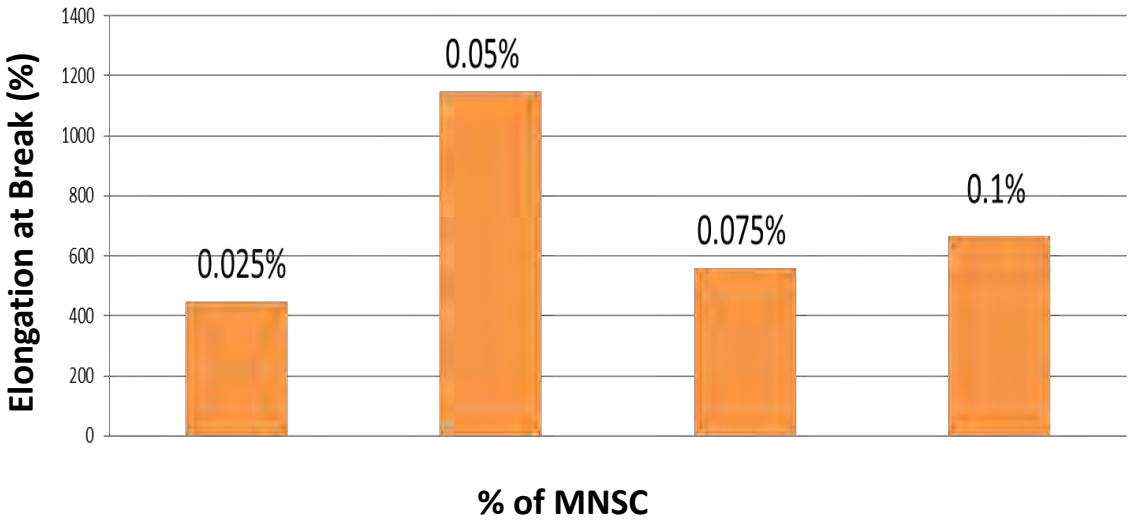

Fig. 3.17: Elongation at break of MNSC-NIPA hydrogel

Table 3.5: Elongation at break for MNSC-NIPA hydrogel

Amount of Cross-linker (% CL)	Elongation at Break (%)
0.025	446
0.05	1147
0.075	557
0.1	667

At lower concentration of MNSC, MNSC-NIPA hydrogel exhibits brittle fraction, therefore the elongation at break is low. On the other hand, when amount of cross-linker is increased the hydrogels exhibit rubber like behavior. The elongation at break is much higher when used 0.05% cross-linkers for hydrogel. The elongation at break is 1147% which is totally different from other amounts of cross-linking hydrogel. It shows higher elongation at break and also shows higher rubber like behavior. So, using 0.05% amount of MNSC, MNSC-NIPA hydrogel shows highest elongation at break than others. Fig 3.15 shows that using 0.025% MNSC cross-linker the hydrogel is soft, elongation at break is low. The amount of 0.05% cross-linker forms a relatively tough hydrogel.

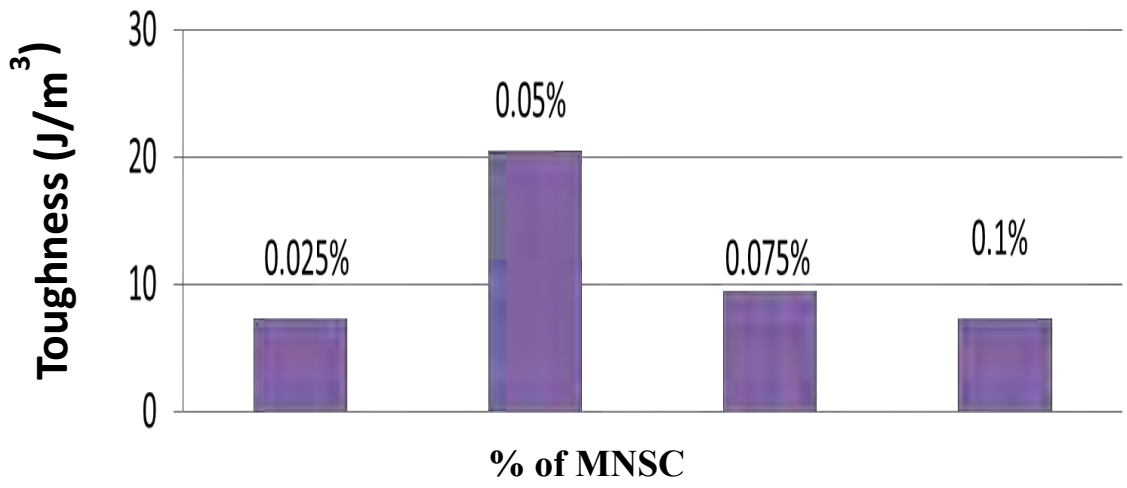

Fig. 3.18: Toughness of MNSC-NIPA hydrogel for elongation

Table 3.6: Toughness for MNSC-NIPA hydrogels

MNSC (%)	Toughness (J/m^3)
0.025	7.39
0.05	20.53
0.075	9.45
0.1	7.30

Toughness is the ability of a material to absorb energy without rupturing. It is usually measured by the energy absorbed in a notch impact test, but the area under the tensile stress-strain curves also give toughness.. Fig 3.15 shows that for the amount of 0.05% MNSC cross-linker elongation area is highest than others and gives highest toughness. It may be attributed to the different network nature among four types of cross-linker concentration of MNSC-NIPA hydrogels. Using 0.025% cross-linker, MNSC-NIPA hydrogel shows low strength, low toughness. Using 0.05% cross-linker, MNSC-NIPA hydrogel shows medium strength and high toughness which is obtained from large stress-strain area. Using 0.075% cross-linker, MNSC-NIPA hydrogel shows high strength and medium toughness. Using 0.1% cross-linker, MNSC-NIPA hydrogel shows high strength and low toughness which are readily determined from stress-strain curve.

3.9.2 Mechanical Properties of MNSC-NIPA hydrogels for compression

Compression test is a technique that is used to examine the mechanical properties of several type of hydrogel [24]. This technique involves placing the material between two parallel plates and compressing it. Fig 3.19 shows that the pressure applied to the surface of the hydrogel and distance the hydrogel is compressed can be used to calculate the mechanical properties of the hydrogel from stress-strain curve.

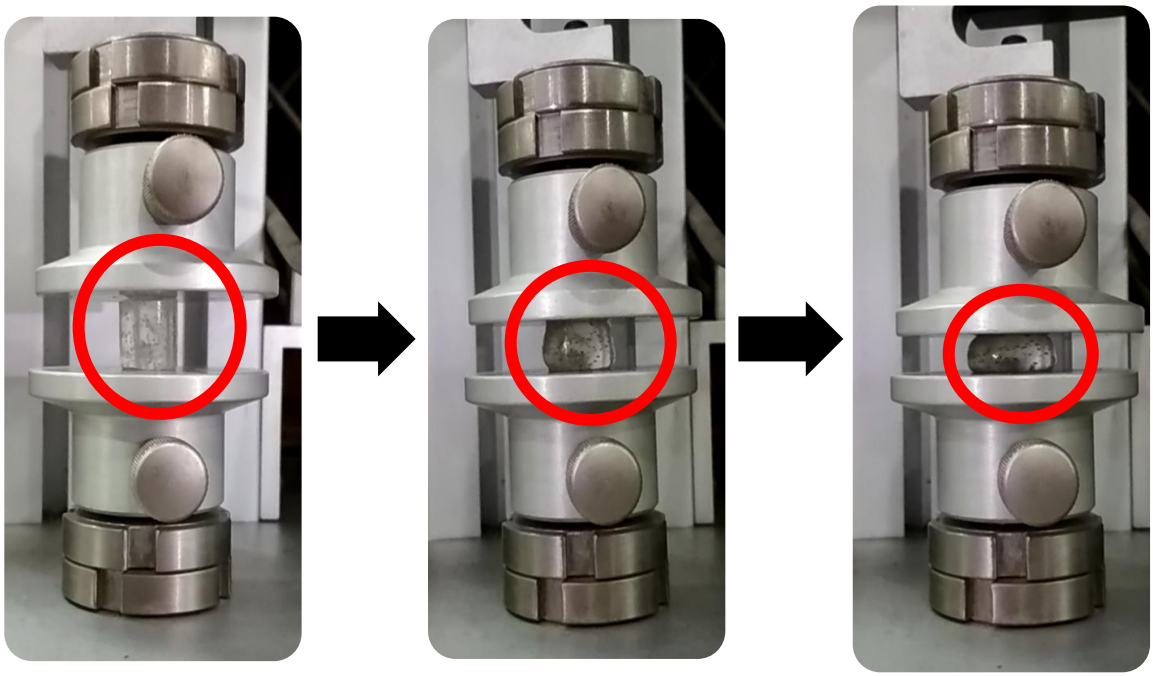

Figure 3.19: Compressive test of MNSC-NIPA hydrogel

To confirm the accuracy of comparison cylindrical hydrogel were made applying same pressure in order to measure compressive strength. The results are also presented in more detail in separate figures. Compressive stress (Mpa) vs strain% curves are depicted in Fig. 3.20. The Figure clearly shows that the increasing amount of cross-linker in the polymer matrix increased the compressive strength as well as the strain. Mechanical properties of different amount cross-linkers are cross-linked in NIPAAM hydrogels as represented in the Figure 3.20.

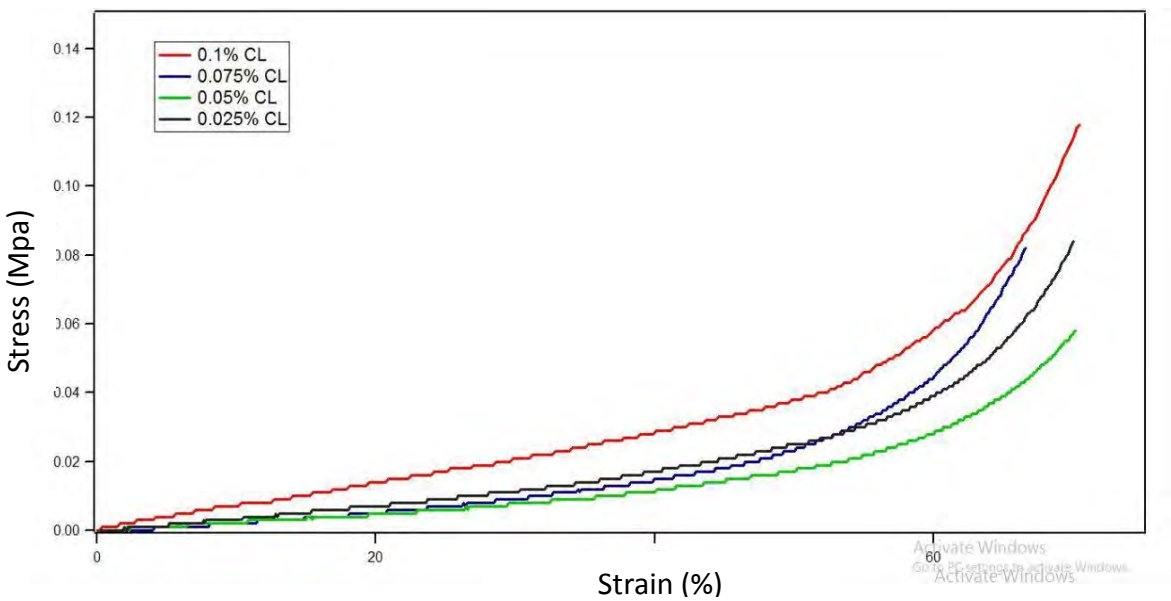

Fig. 3.20: Compressive stress-strain curve MNSC-NIPA hydrogel

In this case no specific numerical stress and strain data are found. The mechanical performance of cross-linked polymer is expected to depend on the formation of covalent bond between cross-linker and polymer matrix. Amount of 0.1% cross-liker hydrogel exhibits at least two times greater mechanical strength than 0.025% cross-linker hydrogel.

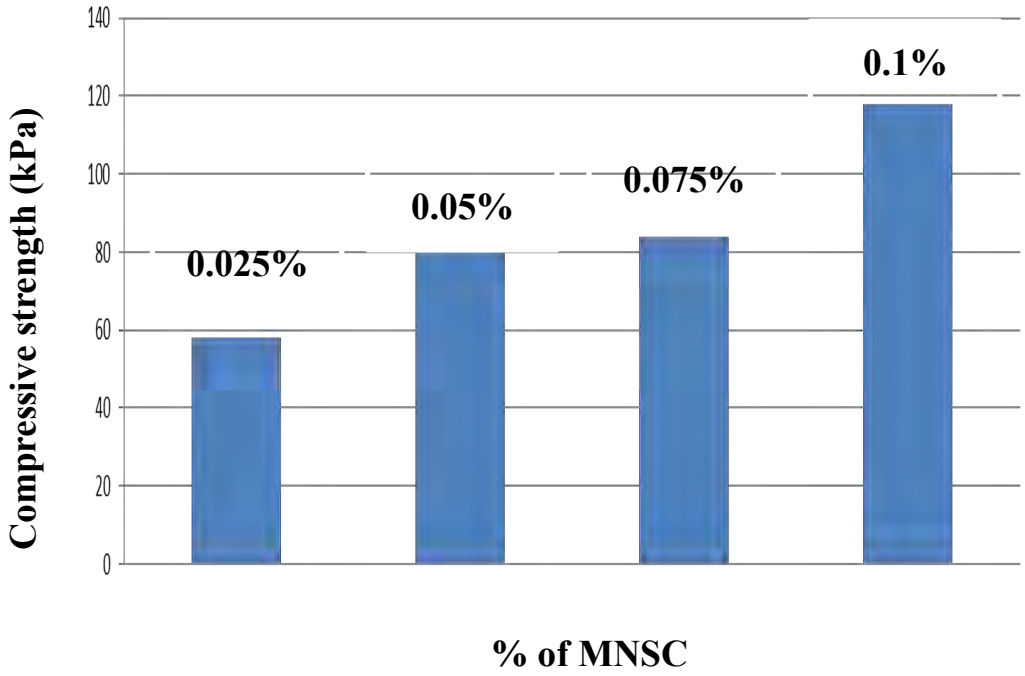

Fig.3.21: Compressive Strength of MNSC-NIPA hydrogel

Table 3.7: Compressive strength of MNSC-NIPA hydrogel

Amount of MNSC (%)	Compressive Strength (kPa)
0.025	58
0.05	81
0.075	84
0.1	118

When load is applied on the hydrogel, the total energy can be dissipated throughout the homogeneously distributed hydrogel network. Fig.3.21 shows that the compressive strength of the hydrogel is 58, 81, 84 and 118 kPa using 0.025%, 0.05%, 0.075% and 0.1% MNSC, respectively. With increasing cross-linker concentration leads to the enhancement in the compressive strength. The compressive stresses for all hydrogel samples are measured after 70% compressive deformation of initial length. Fig. 3.22 shows that Young‟s moduli are approximately same for 0.025% and 0.05% cross-linker hydrogel. But using 0.075% and 0.1% cross-liker, the Young‟s modulus of hydrogel increases drastically.

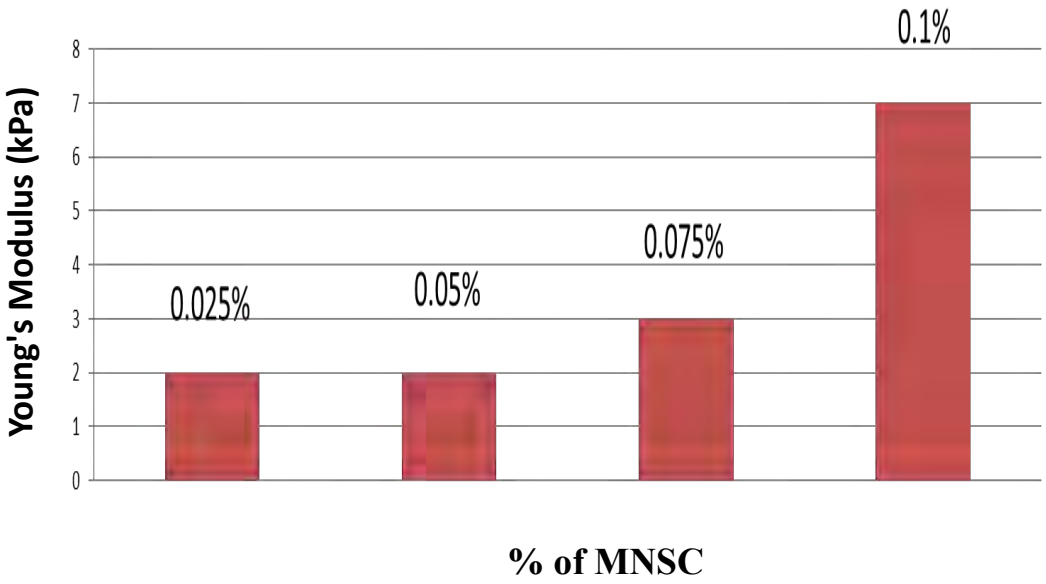

Figure 3.22: Young‟s Modulus of MNSC-NIPA hydrogel during compressive

Table 3.8: Young‟s Modulus of MNSC-NIPA hydrogel

MNSC (%)	Young‟s Modulus (kPa)
0.025	2
0.05	2
0.075	3
0.1	7

Finally we see that Young‟s modulus and compressive strength are dramatically changed with changing cross-linker amount.

Toughness is the ability to absorb energy up to fracture. Total amount of energy absorption can be calculated from the total area of stress-strain curve before fracture. Fig 3.23 shows that toughness of hydrogel increases due to increasing amount of MNSC cross-linker. The higher stress-strain curve area is obtained 0.1% MNSC-NIPA hydrogel which is about 1.5 times higher than uses 0.025% MNSC-NIPA hydrogel.

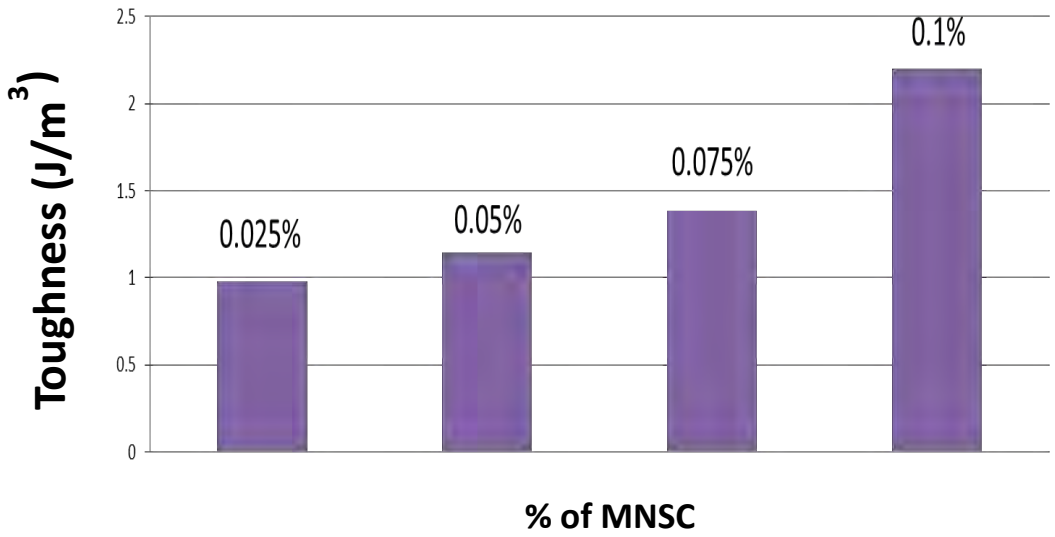

Figure 3.23: Toughness of MNSC-NIPA hydrogel for compressive

Table 3.9: Toughness for MNSC-NIPA hydrogel

MNSC (%)	Toughness (Jm^{-3})
0.025	0.98128
0.05	1.14423
0.075	1.38568
0.1	2.2009

Cross-linker connects one polymer to other via covalent bond. Cross-linking agent changes a liquid polymer into solid or gel by restricting their movement. When amount of cross-linker is increased, the hydrogel network density becomes gradually denser as the extent of compression increased. Thus toughness is enhanced due to increase in the amount of MNSC cross-linker. As a result, the MNSC-NIPA is capable of resisting a great load. Hence, 0.025% MNSC-NIPA hydrogel is less tough than 0.05% MNSC-NIPA hydrogel. Also toughness is gradually increased with increasing amount of cross-linker. The stress, strain and toughness of the MNSC-NIPA gels increase when the cross-linker content is higher, and decreases when the cross-linker content is lower (Fig. 3.20). It perhaps results from the interplay between the covalent cross-linking and the molecular weight of the MNSC-NIPA polymer network. Under deformation, the covalently cross-linked network remains intact to absorb and redistribute the applied stress and thus delay the crack propagation consequently maintain the original configuration. A higher cross-linker content means more cross-linking, and it can effectively absorb and redistribute more applied stress. We see that increasing cross-linker content may induce enhanced mechanical properties. The enhanced strength, toughness and Young‟s modulus of the MNSC-NIPA hydrogels at high cross-linker content are attributed to a highly dense covalently cross-linked network within homogeneous cross-linking points and short network chains of the polymer [25].

References:

[1] Kumar, A., Negi, Y. S., Choudhary, V., Bhardwaj, N. K., "Characterization of cellulose nanocrystals produced by acid-hydrolysis from sugarcane bagasse as agro-waste", *J. Mater. Physic. Chem.*, Vol. 2 (1), pp. 1-8, 2014.

[2] Huang, F. Y., Wu, X. J., Yu, Y., and Yan-Hua Lu, Y. H., "Preparation and Properties of Cellulose Laurate (CL)/Starch Nanocrystals Acetate (SNA) Bio-nanocomposites" *Polymers,* Vol. 7, pp. 1331-1345, 2015.

[3] Ramström, O., and Yan M., "Glyconanomaterials for combating bacterial infections." *Chem-Eur. J.,* Vol. 21(46) pp. 16310-16317, 2015.

[4] Elazzouzi-Hafraoui, S., Nishiyama Y., et al. "The shape and size distribution of crystalline nanoparticles prepared by acid hydrolysis of native cellulose." *Biomacromolecules,* Vol.9.1 pp. 57-65, 2007.

[5] Xiao, B., Sun, X. F., and Sun, R, C,. "Chemical, structural, and thermal characterizations of alkali-soluble lignins and hemicelluloses, and cellulose from maize stems, rye straw, and rice straw," *Polym. Degrad. Stabil.,* Vol. 74.2 pp. 307-319. 2001.

[6] Kim, H. Y., Park, D. J., Kim, J. Y., and Lim, S. T., "Preparation of crystalline starch nanoparticles using cold acid hydrolysis and ultrasonication", *Carbohyd. Polym*., Vol. 98, pp. 295-301, 2013.

[7] Kim, H. Y., Hax, J. A., "Effect of ultrasonic treatments on nanoparticle preparation of acid hydrolyzed waxy maize starch," *Carbohyd. Polym.,* Vol. 93, pp. 582-588, 2013.

[8] Katoa, Y., Matsuoa, R., Isogaib A., "Oxidation process of water-soluble starch in TEMPO-mediated system," *Carbohyd. Polym.,* Vol. 51 pp. 69-75, 2003.

[9] Saito, T., Kimura, S., Nishiyama, Y., and Isogai, A., "Cellulose Nanofibers Prepared by TEMPO-Mediated Oxidation of Native Cellulose," *Biomacromolecules,* Vol. 8.8, pp. 2485-2491, 2007.

[10] Herrmann, W. A., Rost, A. M. J., Tosh, E., Rieplb, H and Kuhn, F. E., "Super absorbers from renewable feedstock by catalytic oxidation," Vol. 10, pp. 442-446, 2008.

[11] Erdem, K., Torbjo, P., Mikael, A., and Lars, W., "Adhesive Layer-by-Layer Films of Carboxymethylated Cellulose NanofibrilDopamine Covalent Bioconjugates Inspired by Marine Mussel Threads," *Karbulutetal.*, Vol. 6, pp. 4731–4739, 2012.

[12] Duan, B., Sun, P., Wang, X., and Yang, C., "Preparation and properties of starch nanocrystals carboxymethyl chitosan nanocomposite flims," *Starch-Starke*, Vol.63, pp, 528-535.

[13] Navaee, A., and Salimi, A., "Efficient amine functionalization of graphene oxide through the Bucherer reaction: an extraordinary metal-free electrocatalyst for the oxygen reduction reaction," *RSC Advances*, Vol. 5, pp. 59874-59880, 2015.

[14] Chakraborty, S., Saha, S., Dhanak, V. R., et al., "High yield synthesis of amine functionalized graphene oxide and its surface properties," *RSC Advances*, Vol. 6, pp. 67916-67924, 2016.

[15] Lai, L., Chen, L., Zhan D., et al., "One-step synthesis of NH_2-graphene from in situ graphene-oxide reduction and its improved electrochemical properties," *Carbon,* Vol. 49, pp. 3250-3257, 2011.

[16] Hu, Y. F., Zhang, X. D., et al., "Selective Oxidation of Corn Starch in TEMPO-Mediated System" *Adv. Mat. Res.,* Vol. 1051, pp.221-224, 2014.

[17] Zhang, W., Ma J., Gao, D., et al., "Preparation of amino-functionalized graphene oxide by Hoffman rearrangement and its performances on polyacrylate coating latex*," Prog. Org. Coat.,* Vol. 94, pp. 9-17, 2016.

[18] Pong, F. Y., Lee, M., Bell, J. R., et al., "Thermoresponsive Behavior of Poly(N-Isopropylacrylamide) Hydrogels Containing Gold Nanostructures" *Langmuir,* Vol. 22, pp. 3851-3857, 2006.

[19] Zhu, X., Gu, X., Zhang, L., and Kong, X, Z., "Preparation and characterization of nanosized P(NIPAM-MBA) hydrogel particles and adsorption of bovine serum albumin on their surface" *Nano scale Res. Lett.,* Vol. 7(1), pp. 1-8, 2018.

[20] Tang, S., Floy, M., Bhandari, R., Sunkara, M., et al., "Synthesis and Characterization of Thermoresponsive Hydrogels Based on N-Isopropylacrylamide Crosslinked with 4,4′- Dihydroxybiphenyl Diacrylate" *ACS Omega,* Vol. 2, pp. 8723−8729, 2017.

[21] Drury J. L., Dennis R. G., Mooney D. J., The tensile properties of alginate hydrogels. *Biomaterials*, Vol. 25, pp. 3187-3199, 2004.

[22] Svensson A., Nicklasson E., Harrah T., Panilaitis B., Kaplan D. L., Brittberg M., Gatenholm P., "Bacterial cellulose as a potential scaffold for tissue engineering of cartilage," *Biomaterials,* Vol. 26, 419-431, 2005.

[23] Zhong, M., Liu, Y. T., Liu, X. Y., et al., "Dually cross-linked single network poly(acrylic acid) hydrogels with superior mechanical properties and water absorbency," *Soft Matter,* Vol. 12, pp. 5420-5428, 2016.

[24] Jeffrey, L., Hinkley, A., Morgret, L. D., Gehrke, S. H., "Tensile properties of two responsive hydrogels", *Polymer*, Vol. 45 pp.8837-8843, 2004.

[25] Awad, H. A., Quinn, W. M., Leddy, H.A., Gimble, J.M., Guilak, F., "Chondrogenic differentiation of adipose-derived adult stem cells in agarose, alginate and gelatin scaffolds", *Biomaterials,* Vol. 25 pp.3211-3222, 2004.

CHPTER 4
Conclusion

4 Conclusion:

Nano-starch particles were prepared successfully with high yield (70%) by hydrolysis method using 18% (w/w) H_2SO_4 solution. The size of fabricated MNSC cross-linker are in nano scale dimension and uniform in size. The presence of C, O and N containing functional groups in the MNSC cross-linker are confirmed by EDS analysis. Carbamide bond are formed between MNSC and 2-AEM which is confirmed by the presence of N containing functional groups. Thermoresponsive MNSC-NIPA hydrogel is successfully synthesized by free radical polarization of NIPAAM monomer in presence of MNSC cross-linker. Remarkable mechanical properties such as tensile strength, Young‟s modulus, ductility and toughness are observed during both compression and elongation test of hydrogel. Elongation at break (%) of 0.05% MNSC-NIPA hydrogel is 1147% where 0.025% MNSC-NIPA hydrogel is only 446%. The compressive strength of the MNSC-NIPA hydrogel is 58, 81, 84 and 118 kPa for 0.025%, 0.05%, 0.075% and 0.1% MNSC-NIPA hydrogels, respectively. The mechanical properties are highly enhanced due to increased amount of MNSC for both compressive and elongations tests which are investigated from stress-strain curves. The MNSC-NIPA hydrogel prepared using 0.05% crosslinking agent exhibits highest elongation at break. The fabricated MNSC-NIPA hydrogel is highly stretchable, ductile and tough. Interestingly, these mechanical properties can be tailored by varying amount of cross-linker and monomer.